European Journal of Medicinal Chemistry xxx (2016) 1–15

Contents lists available at ScienceDirect

European Journal of Medicinal Chemistry

journal homepage: http://www.elsevier.com/locate/ejmech

Research paper

Integrated bioinformatics, computational and experimental methods to discover novel Raf/extracellular-signal regulated kinase (ERK) dual inhibitors against breast cancer cells

Yin Chen [a, 1], Yaxin Zheng [a, 1], Qinglin Jiang [a, b, 1], Feifei Qin [a], Yonghui Zhang [c], Leilei Fu [a, *], Gu He [a, **]

[a] State Key Laboratory of Biotherapy/Collaborative Innovation Center for Biotherapy, West China Hospital, West China Medical School, Sichuan University, Chengdu 610041, China
[b] School of Pharmacy and Sichuan Province College Key Laboratory of Structure-Specific Small Molecule Drugs, Chengdu Medical College, Chengdu 610500, China
[c] Collaborative Innovation Center for Biotherapy, School of Medicine, Tsinghua University, Beijing 100084, China

ARTICLE INFO

Article history:
Received 30 June 2016
Received in revised form
4 November 2016
Accepted 5 November 2016
Available online xxx

Keywords:
Breast cancer
Raf
ERK
Bioinformatics
Kinase inhibitor

ABSTRACT

Beginning with our previously reported ERK inhibitor BL-EI001, we found Raf1 to be an important regulator in the ERK interactive network, and then we designed and synthesized a novel series of Raf1/ERK dual inhibitors against human breast cancers through integrative computational, synthetic and biological screening methods. Moreover, we found that compound 9d suppressed the proliferation of breast cancer cell lines and induced cellular apoptosis via a mitochondrial pathway with only partial dependence on Raf1 and ERK. Our results suggest that an integrative method including in silico design, chemical synthesis, biological screening and bioinformatics analysis could be an attractive strategy for the discovery of multi-target inhibitors against breast cancer.

1. Introduction

According to 2015 cancer statistics, breast cancer is expected to account for approximately 29% of all new cancer cases among women and is the second most common cancer worldwide after lung cancer [1]. Breast cancers have become one of the most challenging solid tumors to diagnose and treat due to their heterogeneity. Breast cancers occur with a variety of intra-tumor and inter-tumor genetic and epigenetic alterations, so the detection and validation of biomarkers will greatly assist targeted therapy for breast cancer [2]. A number of studies suggest that the Raf/MEK/ERK signaling pathway is hyperactivated in tumors, and targeting the Raf/MEK/ERK pathway plays an important role in the treatment of breast cancer [3–5]. Mitogen-activated protein kinase (MAPK) cascades are related to the regulation of normal cell proliferation, survival and differentiation, while the inhibitor of the extracellular signal-regulated kinase (ERK) MAPK pathway has been used for the treatment of cancer [6–9]. Recently, the use of Raf or MEK inhibitors targeting ERK signaling has shown promising clinical activity in breast cancer treatment [4,10,11]. Therefore, intrinsic and acquired targeting resistance to the Raf/MEK/ERK signaling pathway would be an innovative approach for breast cancer therapy.

In our previous studies, we have designed and synthesized a novel ERK inhibitor, named BL-EI001, that could induce ERK-dependent mitochondrial apoptosis against breast cancer both in vitro and in vivo [12]. Further studies suggest that apoptosis induced by BL-EI001 is independent of the Ras/Raf/MEK pathway in breast cancer cells. These results indicate the complexity of the kinase signaling network. The proteomics analysis of BL-EI001-treated breast cancer cells indicate some potential ERK interactive proteins in breast cancer cells, such as HMGB1, BIRC6 and ATFM2, among others. Many BL-EI001-regulated ERK interactive proteins interact directly or indirectly with another oncogene family, the Raf

* Corresponding author.
** Corresponding author.
E-mail addresses: leilei_fu@163.com (L. Fu), hegu@scu.edu.cn (G. He).
[1] These authors contributed equally.

http://dx.doi.org/10.1016/j.ejmech.2016.11.009
0223-5234/

protein family, which is not affected by BL-EI001. In the past few years, some researchers have reported that the inhibition of Raf resulted in potent suppression of different kinds of breast cancers [13–18], so we speculate that the simultaneous inhibition of Raf and ERK might be a feasible therapeutic approach for breast cancer.

To our knowledge, several small molecular Raf inhibitors have been approved by the FDA for cancer therapy, e.g., sorafinib [19,20], vemurafenib [21] and dabrafenib [22], among others. Several B-Raf inhibitors are still in the clinical research stage, such as encorafenib [23], CEP-32496 [24] and RO5126766 [25], among others (Fig. 1A). Their lesser development status means that only a few ERK inhibitors have been registered for clinical trials. The first small molecule ERK inhibitor developed was FR180204 [26], with only modest inhibitory activity. Afterwards, several potent ERK inhibitors, such as VTX-11e [27], SCH772984 [28] and ulixertinib [29], were discovered to inhibit ERK with IC_{50} values at the nanomolar level (Fig. 1B). Most recently, Peng et al. reported the design and synthesis of a novel pan-Raf inhibitor, LY3009120, which bound to both the activated monomer or homodimer of B-Raf and the Ras-dependent heterodimer of B-Raf and Raf1 [30]. Peng et al. suggested that the unique binding modes of the potent Raf1 inhibitor LY3009120 to the RAF kinase domain were responsible for its effectiveness against both B-Raf and Ras mutant cancer cells. It is apparent that a Raf/MEK/ERK pathway inhibitor could be more effective than the current monomeric and dimeric B-RAF inhibitors [31,32]. Therefore, the discovery of novel Raf/ERK dual inhibitors and the validation of their detailed molecular mechanisms are feasible research avenues in breast cancer therapy.

Although several compounds have been reported to possess non-specific multiple inhibitory activities against both Raf and ERK, to our knowledge, there have been few reports of successful Raf1/ERK dual inhibitors for breast cancer therapy. In the current study, we designed and synthesized a series of 4-pyrimidinyl-*N*-arylureas as novel Raf1/ERK dual inhibitors. These compounds potently suppressed the kinase activities of both Raf1 and ERK (Fig. 1C). The IC_{50} values of the most potent compound, 9d, were at the submicromolar level. Herein, we utilized integrated proteomics, computational and experimental methods to discover novel Raf1/ERK dual inhibitors as potential breast cancer therapeutics via inducing apoptosis. The new leads show no apparent toxicity and are suitable for further development for breast cancer therapy.

2. Results and discussion

2.1. Raf is an important regulator in the ERK interactome

Based on the online protein-protein interaction (PPI) databases, we computationally constructed a global human PPI network covering almost all PPIs. We derived physical protein–protein interactions from manually created PPI databases to construct the set

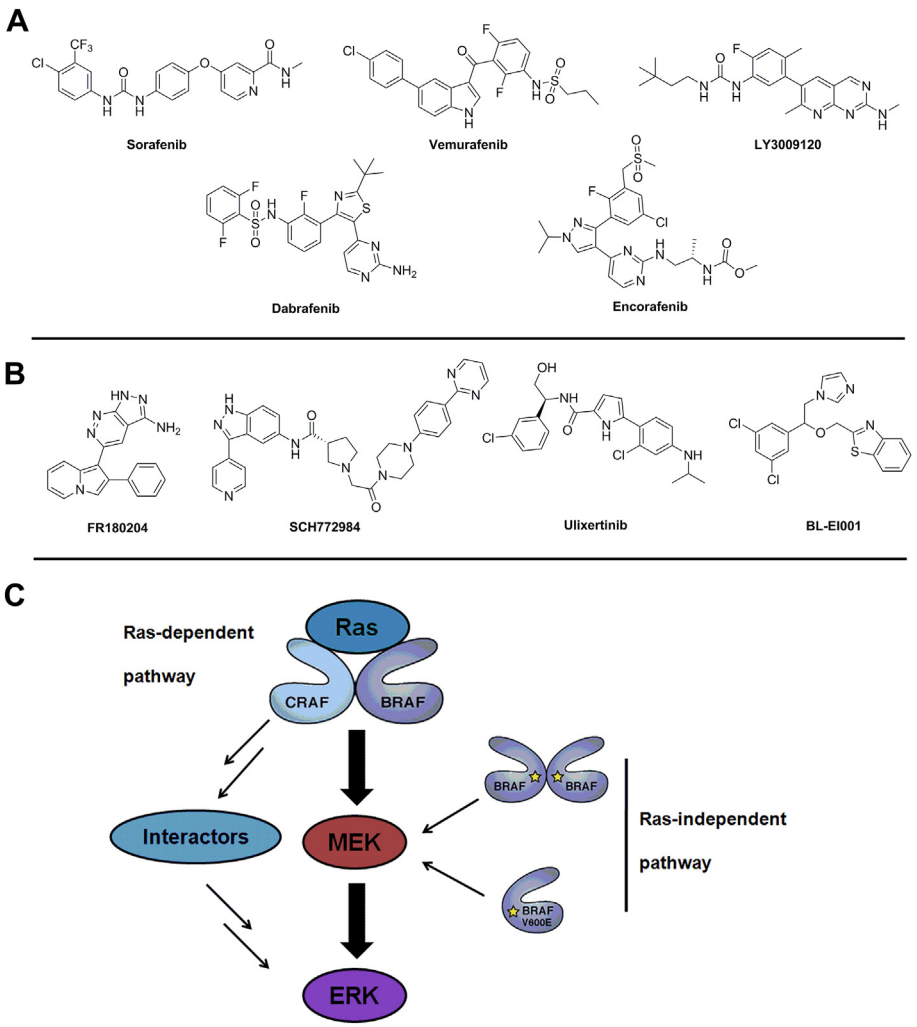

Fig. 1. Chemical structures of selected Raf inhibitors (A), ERK inhibitors (B) and the Ras-dependent or Ras independent mechanism of Raf-ERK pathways (C).

Please cite this article in press as: Y. Chen, et al., Integrated bioinformatics, computational and experimental methods to discover novel Raf/extracellular-signal regulated kinase (ERK) dual inhibitors against breast cancer cells, European Journal of Medicinal Chemistry (2016), http://dx.doi.org/10.1016/j.ejmech.2016.11.009

of true-positive gene pairs, including 14,892 from Homo MINT among 6240 proteins [33]; 39,044 from HPRD among 9619 proteins [34]; 37,710 from BioGRID among 8982 proteins [35]; 8044 from BOND among 4073 proteins [36]; and 34,935 from IntAct among 8849 proteins [37]. Subsequently, we modified this network into a RAF/MEK/ERK sub-network including 812 nodes and 929 edges. Moreover, we constructed a proteomics-based RAF/ERK-modulated PPI network based on BL-EI001-treated MCF-7 cells, including 95 differentially expressed proteins and 132 interactions. Notably, we found that 18 ERK1 interactors were regulated by RAF1, and 38 RAF1 interactors were regulated by ERK1 (Fig. 2). Thus, these results showed that RAF/MEK/ERK-independent pathways in breast cancer may regulate the process of apoptosis.

2.2. Raf1 and ERK1 are highly homologous in the kinase domain

The sequence alignment of Raf1 and ERK1 is shown in Fig. S1. The relatively low sequence identity (approximately 20% identity) and sequence similarity (approximately 48% similarity) in the two proteins were due to the four additional loops in Raf1. The sequence identity between Raf1 and ERK1 increased from 20% to 46% if the additional loops in Raf1 were excluded. According to the superposed structures of the two proteins (Fig. S2), the four additional loops were not adjacent to the inhibitor binding pocket. Moreover, the binding modes of Raf1 and ERK1 with their inhibitors were similar (Figs. S3A and B). The main difference was that the pocket of Raf1 was more open and formed a cramped groove for tight binding of the inhibitor, whereas the pocket of ERK1 was constricted and only allowed smaller inhibitors.

2.3. Design and synthesis of novel Raf1/ERK dual inhibitors

To identify novel Raf1/ERK dual inhibitors for overcoming the intrinsic or acquired resistance of breast cancer cells against the current B-Raf inhibitors, we blended the structural features of several pan-Raf inhibitors and ERK inhibitors based on their co-crystallographic binding modes (Scheme 1). Compound **7a** was first discovered to inhibit both Raf1 and ERK with IC_{50} values at the micromolar level (Table 1).

The synthesis route of compounds **7a-l**, **8a-h**, **9a-g** and **10a-c** is shown in Scheme 2. In general, commercially available compound 1 was coupled with 4,6-dichloropyrimidine under base catalysis to produce compound **2**. Then, the nitrogen group of compound **2** was reduced to an amino group by iron powder to produce compound 3.

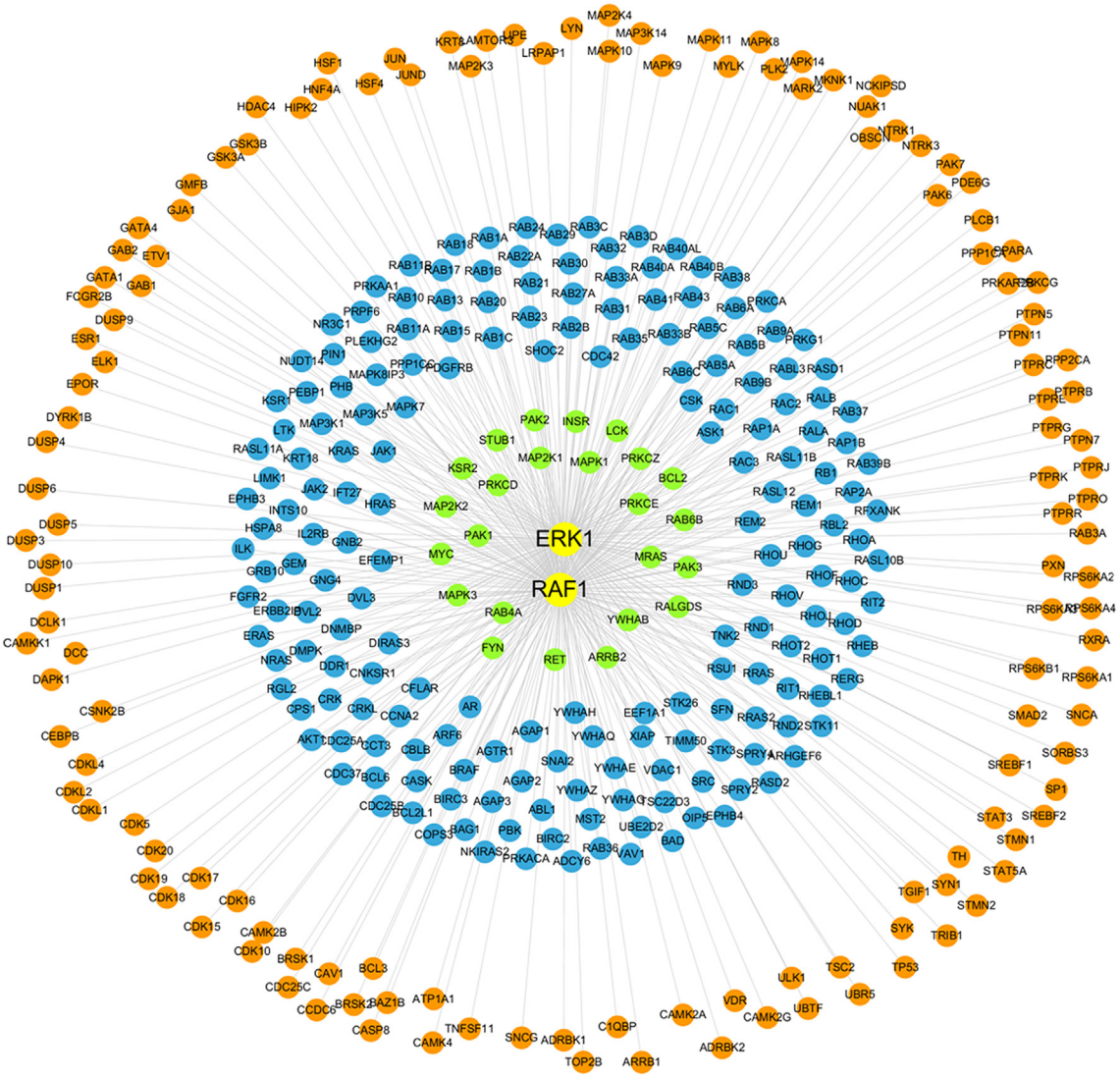

Fig. 2. The interactors between Raf and ERK.

Please cite this article in press as: Y. Chen, et al., Integrated bioinformatics, computational and experimental methods to discover novel Raf/extracellular-signal regulated kinase (ERK) dual inhibitors against breast cancer cells, European Journal of Medicinal Chemistry (2016), http://dx.doi.org/10.1016/j.ejmech.2016.11.009

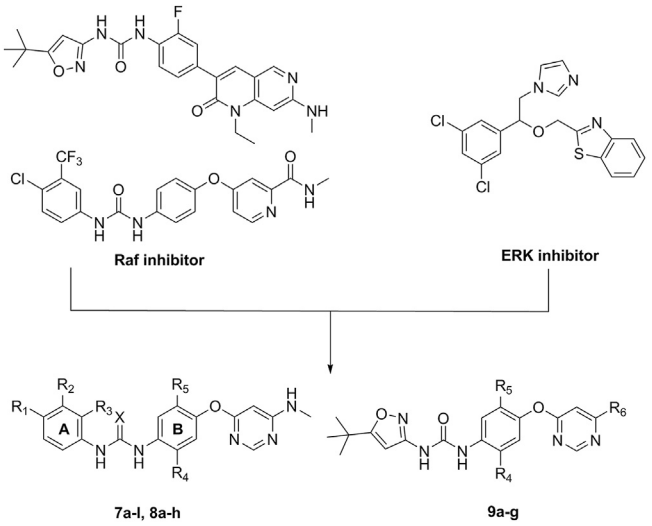

Scheme 1. Strategy for the design of novel Raf/ERK dual inhibitors.

The 6-chloro atom on the pyrimidine ring of compound 3 was reacted with a series of secondary amines to produce compounds **4a-h**. Finally, the reactions between compound 4 and different isocyanate, isothiocyanate or in situ generated isocyanate produced the target compounds 7a-l, 8a-h, **9a-g** and **10a-c**. All compounds were fully characterized by ^{1}H NMR, ^{13}C NMR and high-resolution mass spectrometry.

2.4. Novel Raf1/ERK dual inhibitors possess good kinase selectivity and suppress breast cancer cell proliferation

Structural optimizations of the lead compounds **7a** and **9a** were conducted to improve their inhibitory capacity against Raf1 and ERK. The kinase inhibitory and cellular proliferation assay results are shown in Table 1. The analysis of the structure-activity relationship was mainly focused on the influences of various substituent groups at the following three groups (Scheme 2) on the dual ERK and Raf1 inhibitory activities: the aromatic ring of the urea or thiourea (Ring A), the substituents of the phenyl ring B (R_4 and R_5), and the 6-substituents of the pyrimidine ring (R_6).

First, we investigated the influence of the substitute groups in aromatic ring B of compound **7** on its inhibitory capacity against Raf1 and ERK kinases via the addition of a fluorine atom or methyl group. The results suggested that the position of the substitute groups in aromatic ring B possessed diverse effects on the inhibitory activity against ERK and Raf1. Two substituents were used in the SAR studies: a fluorine or methyl group in R_4, and a methyl group in R_5. Larger substituents were limited by the steric hindrance of phenyl ring B. Larger substituent groups, e.g., bromide, enthyl or trifluoromethyl group could dramatically reduce the productivity of the target compounds. It was apparent that the introduction of a methyl group at the R_4 position led to a moderate increase in bioactivities in both the kinase and cell proliferation assays. Second, we explored the influences of different substituents on aromatic ring A by setting the phenyl ring as its original group and varying R_1, R_2 and R_3. The kinase and cell proliferation inhibitory activities of the thiourea-linked compounds (**8a-h**) are shown in Table 1. It was apparent that the 3-CF_3, 4-Cl phenyl substituents had better activities than the other groups. In addition, comparison of the urea-linked compounds (**7a-l**) and thiourea-linked compounds (**8a-h**) indicated that the urea linker was slightly better than the thiourea. In the urea-linked compounds, the 3-CF_3,4-Cl phenyl substituent in aromatic ring A also displayed preferential bioactivities. Furthermore, some other substituents such as cyclopropane, 2-thiazolyl, and 2-benzothiazolyl were introduced (**10a-c**), but these compounds only showed weak inhibitory potency in both kinase and cytotoxicity assays. Finally, the 5-tBu-isoxazole substitute was discovered as a fragment with a potent effect on Raf. This fragment was then coupled with compound 4 (**9a-g**) [38–41]. The bioactivity results of compound **9** suggested that the 5-tBu-isoxazole substituent displayed stronger activities than the 3-CF_3, 4-Cl phenyl substituents for aromatic ring A.

To determine the influences of substituents at the 6-position of the pyrimidine moiety, several substituents were introduced to replace the methylamino group. Compared to **9a** and **9d**, the substitution of R_6 by morpholino or piperidine-1-yl groups displayed marginal influences on the inhibitory effects against Raf1 kinase and decreased the inhibitory activities against ERK kinase and cell proliferation in MCF-7 and MD-MBA-231 cells. The cell proliferation assay also revealed that these compounds indeed displayed stronger inhibition against the growth of MCF-7 cells than MD-MBA-231 cells. Interestingly, only compound 9d strongly suppressed the proliferation of MCF-7 and MD-MBA-231 breast cancer cells with the lowest IC_{50} values of 0.39 and 2.10 μM, respectively. Compound **9d** was thus used in subsequent studies.

The kinase selectivity profile of **9d** was performed on a panel of 100 kinases by using the KINOMEscan assay (Discoverx Co. Ltd., Fremont, CA, USA) at a constant concentration of 1.0 μM. The results demonstrated that compound **9d** could also potently inhibit B-Raf, VEGFR2 and PDGFRβ at the submicromolar level, in addition to its dual targets against Raf1 and ERK. Moreover, further investigation should be performed on the safety of compound **9d** in association with its relatively broad kinase inhibitory profiles (see Table S1). The molecular docking of compound **9d** with the ATP sites of Raf1 and ERK1 was also performed (Figs. S3C and D). In Raf1, **9d** formed stable hydrogen bonds with Glu122 and Met 125 and π-π interactions between Tyr53 and the pyrimidine ring. For ERK1, **9d** could formed hydrogen bonds with Lys431 and strong π-π interactions were observed between Trp423 and Phe475 and the benzene ring.

2.5. Novel dual inhibitor induces apoptosis via the mitochondrial pathway with partial dependence on Raf1 and ERK

Flow cytometry analysis was performed to determine the death subroutine of compound **9d**-treated MCF-7 breast cancer cells using the Annexin V/PI staining kit (Fig. 3). According to Fig. 3, the percentage of apoptotic cells in the **9d** treatment group was 41.2% ± 3.20%, which was significantly higher than in the BL-EI001 group (19.9% ± 1.8%, $p < 0.05$) and the NS (2.5% ± 0.4%, $p < 0.05$) group. There were no significant differences in early apoptosis between the 9d treatment group (5.7% ± 0.6%) and the BL-EI001 (3.3% ± 0.4%) group, but the rate of late apoptotic cells in the **9d** treatment group (35.4% ± 2.8%) was much higher than in the free PTX group (16.5% ± 1.5%, $p < 0.05$). The results clearly demonstrated that apoptotic cell death was initiated by compound **9d** in a concentration-dependent manner. We then investigated the morphological changes of compound 9d-treated MCF-7 cells by Hoechst 33258 staining (see Fig. 4), and apoptotic cell death was clearly observed under fluorescence microscopy. To further validate the dual inhibitory effects and apoptotic mechanism of compound **9d**, we investigated its suppressive capacity on the activation of the MAPK signal pathway and the apoptotic relative proteins in MCF-7 cells bearing both Raf1 and ERK amplification (Fig. 5). As shown in Fig. 5, treatment with compound **9d** indeed decreased the phosphorylation of Raf1 and ERK in MCF-7 cells in a dose-dependent manner, suggesting that compound **9d** could block the MAPK signal pathway. In addition, the total protein levels of Raf1, ERK and

Please cite this article in press as: Y. Chen, et al., Integrated bioinformatics, computational and experimental methods to discover novel Raf/extracellular-signal regulated kinase (ERK) dual inhibitors against breast cancer cells, European Journal of Medicinal Chemistry (2016), http://dx.doi.org/10.1016/j.ejmech.2016.11.009

Table 1
Kinase inhibitory activity against Raf1 and ERK1, and cytotoxicity against MCF-7 and MDA-MB-231 of compounds 7a-l, 8a-h, 9a-g and 10 a-c.

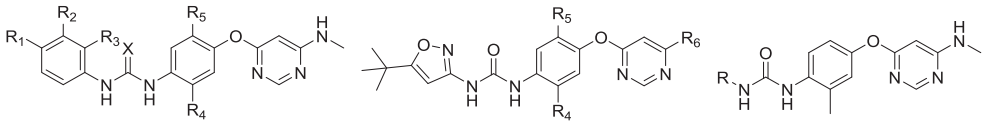

7a-l, 8a-h 9a-g 10a-c

No.	R1	R2	R3	R4	R5	R6	X	Kinase inhibitory (IC_{50}, μM)[a]		Cytotoxicity (IC_{50}, μM)[b]	
								Raf1	ERK1	MCF-7	MD-MBA-231
7a	H	CF_3	H	H	F	–	O	0.169	4.8	0.95	4.27
7b	Br	H	H	H	F	–	O	0.272	7.6	3.30	21.84
7c	MeO	H	H	H	F	–	O	1.80	>10	4.72	13.65
7d	Me	H	H	H	F	–	O	2.30	>10	10.9	>20
7e	Cl	CF_3	H	H	F	–	O	0.099	4.7	0.75	6.98
7f	Cl	H	Cl	H	F	–	O	>10	>10	>20	>20
7g	CF_3	H	H	Me	H	–	O	1.51	>10	15.3	>20
7h	Cl	CF_3	H	Me	H	–	O	0.071	3.1	1.56	5.73
7i	Cl	H	Cl	Me	H	–	O	>10	>10	>20	>20
7j	Cl	H	H	Me	H	–	O	0.67	>10	13.32	>20
7k	MeO	H	H	Me	H	–	O	1.28	>10	15.91	>20
7l	H	Br	H	Me	H	–	O	0.374	>10	5.92	18.67
8a	H	H	H	H	F	–	S	6.20	>10	>20	>20
8b	H	H	H	Me	H	–	S	4.90	>10	>20	>20
8c	Br	H	H	Me	H	–	S	3.05	>10	9.64	>20
8d	H	H	H	H	Me	–	S	7.50	>10	>20	>20
8e	H	CF_3	H	H	F	–	S	2.10	>10	6.84	18.28
8f	H	CF_3	H	Me	H	–	S	1.84	>10	7.26	11.03
8g	Cl	CF_3	H	H	F	–	S	0.86	8.3	2.19	8.27
8h	Cl	CF_3	H	Me	H	–	S	0.77	5.2	1.79	16.73
9a	–	–	–	H	F	Methylamino	–	0.053	1.62	0.56	3.79
9b	–	–	–	H	F	Piperidine-1-yl	–	0.089	7.3	2.70	10.3
9c	–	–	–	H	F	Morpholino	–	0.076	6.9	1.89	15.4
9d	–	–	–	Me	H	Methylamino	–	0.028	0.79	0.39	2.10
9e	–	–	–	Me	H	Morpholino	–	0.051	8.7	0.72	7.39
9f	–	–	–	H	Me	Piperidine-1-yl	–	0.327	>10	4.24	>20
9g	–	–	–	H	Me	Morpholino	–	0.690	>10	3.96	12.3
10a	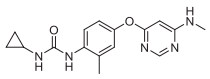							>10	>10	>20	>20
10b	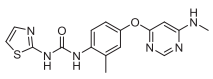							>10	>10	>20	>20
10c	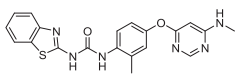							>10	>10	>20	>20

[a] IC_{50} values were determined from KinaseProfiler of Eurofins. The data represent the mean values of two independent experiments.
[b] Each compound was tested in triplicate; the data are presented as the mean values.

GAPDH remained unchanged. To further assess the proteins of the death receptor apoptotic pathway involved in **9d**-treated MCF-7 cells, the levels of Fas, FasL, Fas-Associated protein with Death Domain (FADD) and caspase-8 were determined by Western blot analysis. The results demonstrated that the concentrations of Fas, FasL and FADD were not obviously changed, and nor was the expression level of caspase-8 after compound **9d** treatment (Fig. 5). Simultaneously, the expression level of Bcl-2 declined, whereas Bax expression was increased in MCF-7 cells after treatment with compound **9d**. Moreover, we found enhanced cleavage of caspase-9 in **9d**-induced apoptosis. The total length and cleaved form of caspase-3 were barely observed because of its expression deficiency in MCF-7 cells. These results suggest that the mitochondrial pathway, other than the death receptor, was mainly involved in **9d**-induced apoptosis. These results suggest that the crosstalk between Raf1 and ERK might be a complicated way to follow the classic Raf/MEK/ERK pathway.

3. Conclusions

In conclusion, a series of 4-(pyrimidin-4-yl)oxyl-phenyl-3-arylurea derivatives were discovered as novel dual inhibitors of Raf1 and ERK. Both compounds potently inhibited both kinases with IC_{50} values at the submicromolar level, potently inhibited the proliferation of a panel of breast cancer cells and induced mitochondrial apoptosis. In addition, the most potent compound **9d** demonstrated inhibitory potency of the Raf/MEK/ERK pathway in the MCF-7 cells, suggesting that the Raf1/ERK dual inhibition might be an attractive strategy for breast cancer chemotherapy. Primary molecular mechanism studies of compound **9d** indicated that the individual knockdown of Raf1 and ERK could only partially inhibit its antitumor activity, implying that the direct and indirect

Please cite this article in press as: Y. Chen, et al., Integrated bioinformatics, computational and experimental methods to discover novel Raf/extracellular-signal regulated kinase (ERK) dual inhibitors against breast cancer cells, European Journal of Medicinal Chemistry (2016), http://dx.doi.org/10.1016/j.ejmech.2016.11.009

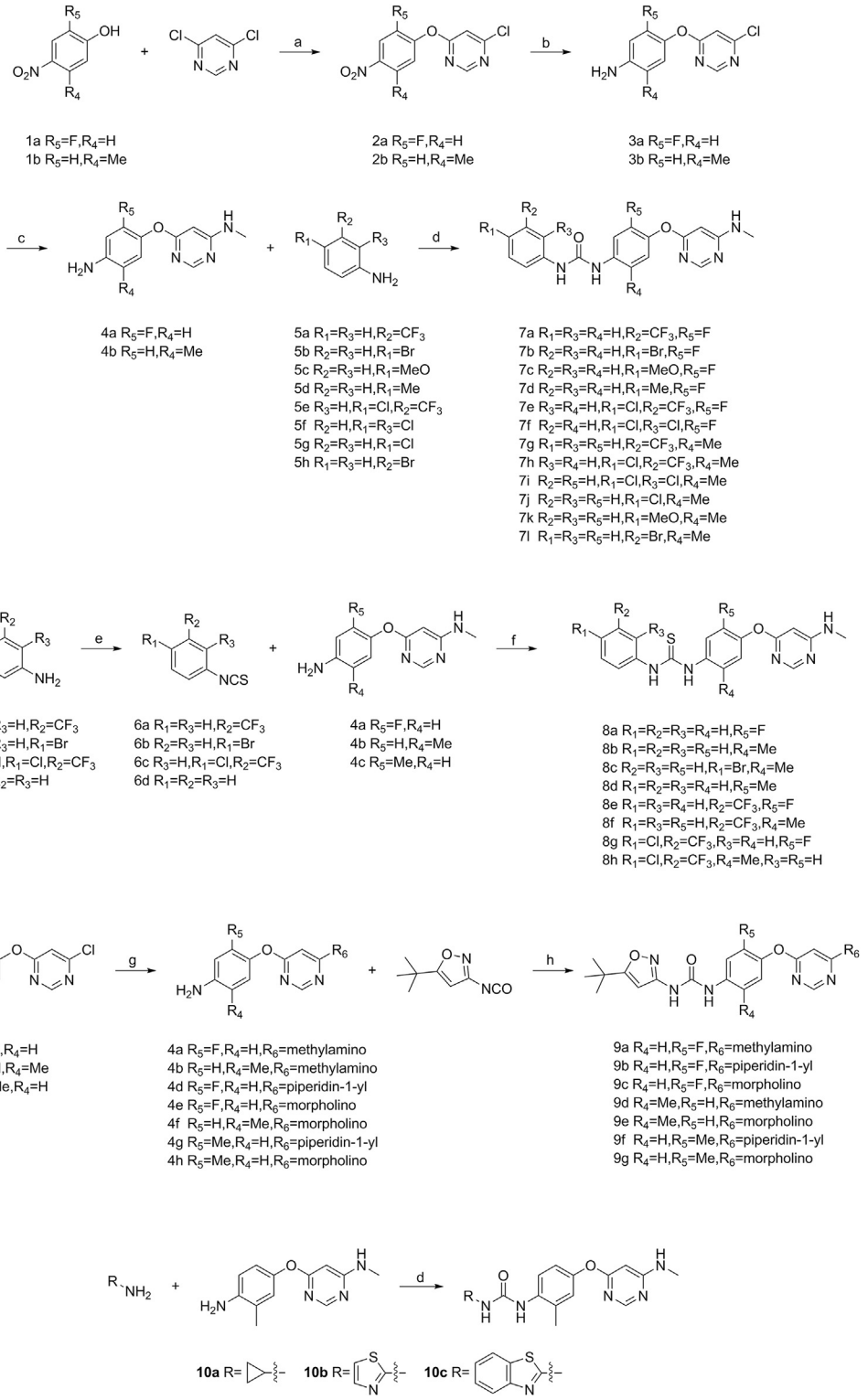

Scheme 2. Reagents and conditions: (a) K_2CO_3, CH_3CN, reflux, 2 h, 54–78%; (b) Fe, NH_4Cl, EtOH, H_2O, reflux, 2 h, 80–88%; (c)CH_3NH_2, 50 °C, 2 h, 45–52%; (d)(i) Triphosgene, Toluene, -5 °C, 1 h, (ii) DCM, rt, 2 h, 54–70%; (e)(i) CS_2, TEA, rt, (ii) $(Boc)_2O$, DMAP, 0°C-rt, 30 min, 48–55%; (f) CH_3CN, rt, 24 h, 63–75%; (g)Morpholine or Piperidine, 50 °C, 2 h, 60–75%.

interactions between Raf1 and ERK were more sophisticated than we previously acknowledged. Taken together, our results indicated that the integrated bioinformatics, computational and experimental discovery of a synthesized Raf1/ERK dual inhibitor was effective for the treatment of breast cancer.

4. Experimental section

4.1. General method

NMR data was obtained for ^1H at 400 MHz, and for ^{13}C at

Please cite this article in press as: Y. Chen, et al., Integrated bioinformatics, computational and experimental methods to discover novel Raf/extracellular-signal regulated kinase (ERK) dual inhibitors against breast cancer cells, European Journal of Medicinal Chemistry (2016), http://dx.doi.org/10.1016/j.ejmech.2016.11.009

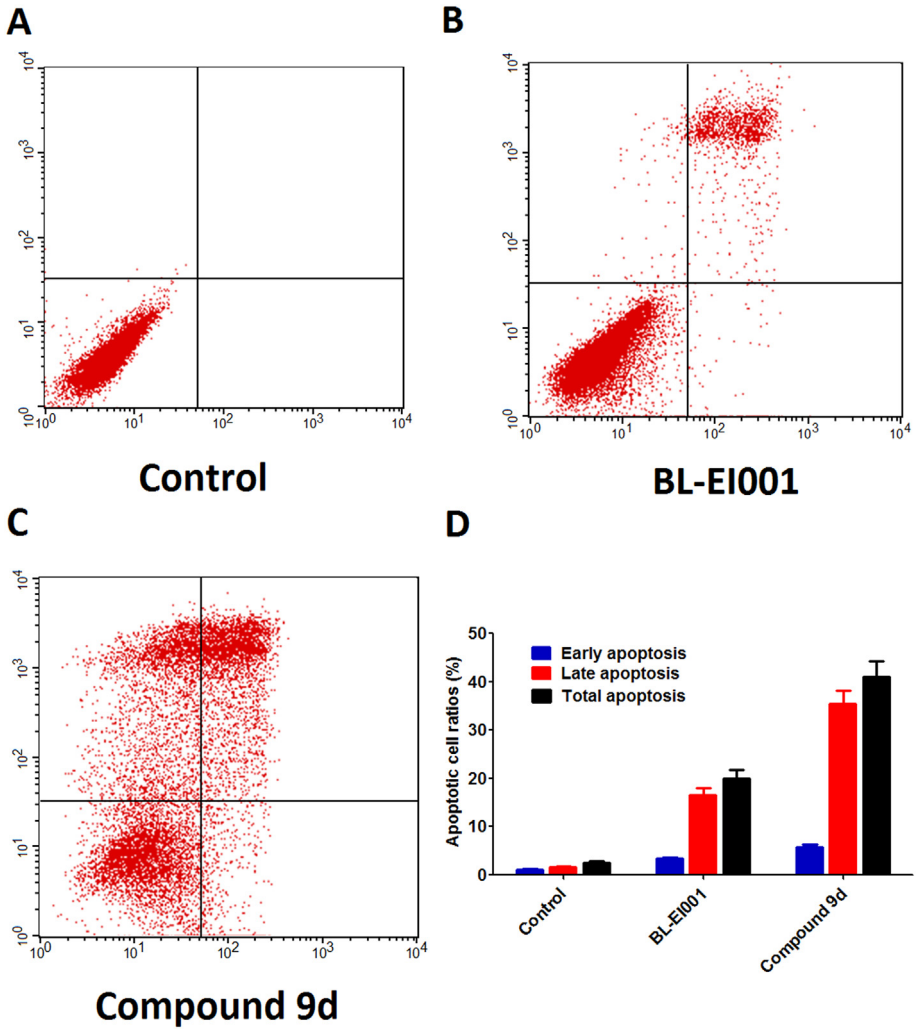

Fig. 3. Apoptosis assay by FCM; (A) Control; (B) BL-EI001; (C) Compound 9d and (D) the quantification of apoptotic cells in each groups.

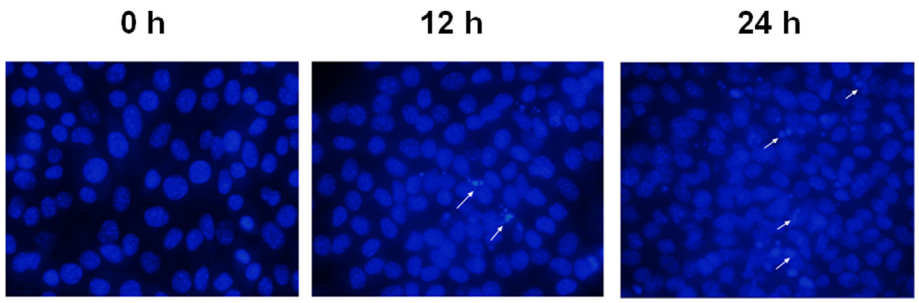

Fig. 4. The cellular morphology was observed without or with 9d treated under fluorescent microscopy after Hoechst 33,258 staining.

100 MHz. Chemical shifts were reported in ppm from tetramethylsilane with the solvent resonance as the internal standard in $CDCl_3$ solution. ESI-HRMS was recorded on a Waters SYNAPT G2 Q-TOF instrument. Column chromatography was performed on silica gel (300–400 mesh) eluting with ethyl acetate and petroleum ether. TLC was performed on glass-backed silica plates. UV light and I_2 were used to visualize products. Melting points were determined on a Mel-Temp apparatus and are uncorrected. All chemicals were used without purification as commercially available unless otherwise noted.

4.2. Synthetic procedures

Genera procedure for the synthesis of 4-chloro-6-(substituted phenoxy)pyrimidines 2a-c.

To a mixture of appropriate phenol (10 mmol) in Acetonitrile (50 mL) was added K_2CO_3 (2.07 g, 15 mmol). The reaction mixture was stirred at room temperature for 10 min. Then 4,6-dichloropyrimidine (1.78 g, 12 mmol) was added to the reaction mixture, followed by heating to reflux for 4 h. The solvent was removed under vacuum. The resulting residue was diluted with

Please cite this article in press as: Y. Chen, et al., Integrated bioinformatics, computational and experimental methods to discover novel Raf/extracellular-signal regulated kinase (ERK) dual inhibitors against breast cancer cells, European Journal of Medicinal Chemistry (2016), http://dx.doi.org/10.1016/j.ejmech.2016.11.009

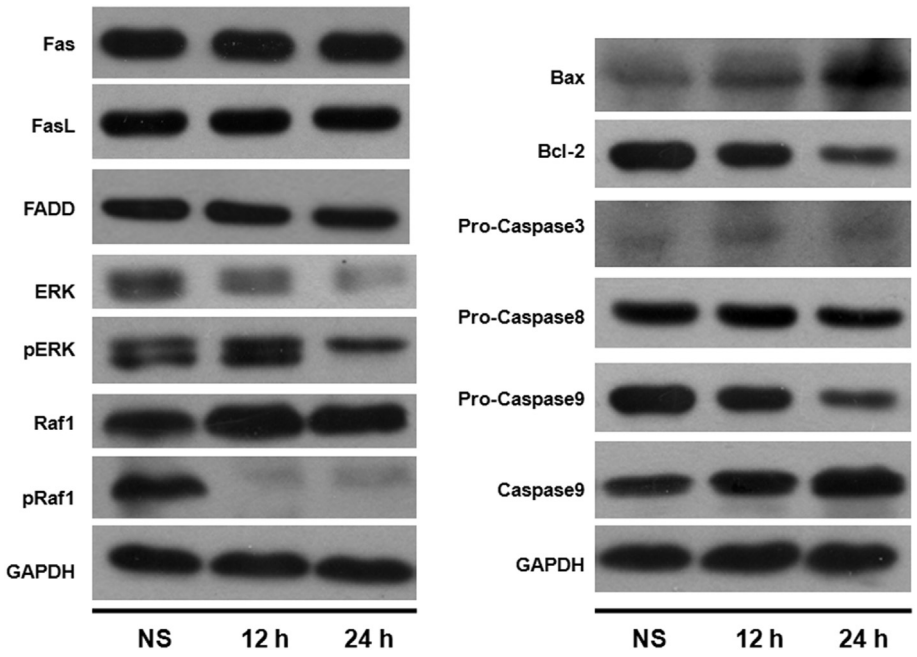

Fig. 5. Western blot analysis of Raf1, ERK and apoptosis related proteins.

water and extracted with ethyl acetate (3 × 30 mL). The combined organic layer was dried over anhydrous sodium sulfate and concentrated under vacuum and then recrystallized from EtOAc and petroleum to afford the product **2a-c**.

4.2.1. 4-Chloro-6-(2-fluoro-4-nitrophenoxy)pyrimidine (2a)

Yield:67%, ^{1}H NMR (Chloroform-d) δ 8.55 (d, J = 0.8 Hz, 1H), 8.18–8.12 (m, 2H), 7.47–7.42 (m, 1H), 7.15 (d, J = 0.8 Hz, 1H).HRMS (ESI) calcd. for $C_{10}H_5ClFN_3NaO_3^+$ $[M + Na]^+$, 291.9896; found, 291.9900.

4.2.2. 4-Chloro-6-(3-methyl-4-nitrophenoxy)pyrimidine (2b)

Yield: 62%, ^{1}H NMR (Chloroform-d) δ 8.55 (d, J = 0.8 Hz, 1H), 8.22 (d, J = 2.4 Hz, 1H), 8.16 (dd, J = 8.8, 2.8 Hz, 1H), 7.24 (d, J = 8.8 Hz, 1H), 7.09 (d, J = 0.8 Hz, 1H), 2.28 (s, 3H). HRMS (ESI) calcd. for $C_{11}H_8ClN_3NaO_3^+$[M + Na]$^+$, 288.0146; found, 288.0141.

4.2.3. 4-Chloro-6-(2-methyl-4-nitrophenoxy)pyrimidine (2c)

Yield: 58%, ^{1}H NMR (Chloroform-*d*) δ 8.55 (d, J = 0.8 Hz, 1H), 8.22 (d, J = 2.4 Hz, 1H), 8.16 (dd, J = 8.8, 2.8 Hz, 1H), 7.24 (d, J = 8.8 Hz, 1H), 7.09 (d, J = 0.8 Hz, 1H), 2.28 (s, 3H).HRMS (ESI) calcd. for $C_{11}H_8ClN_3NaO_3^+$ $[M + Na]^+$, 288.0146; found, 288.0147.

Genera procedure for the synthesis of 4-((6-chloropyrimidin-4-yl)oxy)-3-substituteaniline 3a-c.

To a suspension of 2a-c (5 mmol) in 80% EtOH (40 mL) was added NH_4Cl (1.34 g, 25 mmol) and Fe (1.4 g, 25 mmol). The reaction mixture was heating to reflux for 2 h and then filtered with diatomite. The filtrate was concentrated under vacuum, diluted with water andextracted with ethyl acetate(3 × 30 mL).The combined organic layer was dried over anhydrous sodium sulfate and concentrated under vacuum and then recrystallized from EtOH to afford the product **3a-c**.

4.2.4. 4-((6-Chloropyrimidin-4-yl)oxy)-3-fluoroaniline (3a)

Yield: 75%, ^{1}H NMR (Chloroform-d) δ 8.57 (s, 1H), 6.98–6.94 (m, 2H), 6.51 (dd, J = 12.0, 2.8 Hz, 1H), 6.46 (dd, J = 8.8, 2.8 Hz, 1H), 3.81 (s, 2H).HRMS (ESI) calcd. for $C_{10}H_7ClFN_3NaO^+$ $[M + Na]^+$, 262.0154; found, 262.0157.

4.2.5. 4-((6-Chloropyrimidin-4-yl)oxy)-2-methylaniline (3b)

Yield: 66%, ^{1}H NMR (Chloroform-*d*) δ 8.59 (d, J = 0.8 Hz, 1H), 6.84 (s, 1H), 6.83 (d, J = 0.8 Hz, 1H), 6.80 (dd, J = 8.4, 2.8 Hz, 1H), 6.70 (d, J = 8.4 Hz, 1H), 3.66 (s, 2H), 2.18 (s, 3H).HRMS (ESI) calcd. for $C_{11}H_{11}ClN_3O^+$ $[M + H]^+$, 236.0585; found, 236.0581.

4.2.6. 4-((6-Chloropyrimidin-4-yl)oxy)-3-methylaniline (3c)

Yield: 69%, ^{1}H NMR (Chloroform-*d*) δ 8.59 (d, J = 0.8 Hz, 1H), 6.84–6.82 (m, 2H), 6.60 (d, J = 2.8 Hz, 1H), 6.56 (dd, J = 8.4, 2.8 Hz, 1H), 3.65 (s, 2H), 2.06 (s, 3H).HRMS (ESI) calcd. for $C_{11}H_{11}ClN_3O^+$ $[M + H]^+$, 236.0585; found, 236.0586.

Genera procedure for the synthesis of 6-(4-amino-substituted phenoxy)-aromatic amine 4a-h.

The compound 3a-c (3 mmol) was stirred in 20 mL of tetrahydrofuran at room temperature. To the mixture, 1 mL of 35% methylamine ethanolic solution was added. The resulting mixture was stirred at 45 °C for 4 h. The organic solvent was removed under vacuum and then purified by column chromatography over silica gel to afford compound 4a-h.

4.2.7. 6-(4-Amino-2-fluorophenoxy)-N-methylpyrimidin-4-amine (4a)

Yield: 52%, ^{1}H NMR (Chloroform-*d*) δ 8.22 (s, 1H), 6.96 (t, J = 8.8 Hz, 1H), 6.49 (dd, J = 12.0, 2.8 Hz, 1H), 6.45–6.42 (m, 1H), 5.79 (s, 1H), 5.18 (brs, 1H), 3.74 (s, 2H), 2.90 (d, J = 5.2 Hz, 3H)·^{13}C NMR (Chloroform-*d*) δ 168.98, 164.39, 157.04, 153.94 (d, J = 247 Hz), 144.33 (d, J = 10 Hz), 130.62 (d, J = 13 Hz), 123.26 (d, J = 3 Hz), 109.67 (d, J = 3 Hz), 102.45 (d, J = 22 Hz), 27.43.HRMS (ESI) calcd. for $C_{11}H_{12}FN_4O^+$ $[M + H]^+$, 235.0990; found, 235.0989.

4.2.8. 6-(4-Amino-3-methylphenoxy)-N-methylpyrimidin-4-amine (4b)

Yield: 48%, ^{1}H NMR (Chloroform-*d*) δ 8.24 (s, 1H), 6.84 (d, J = 2.8 Hz, 1H), 6.80 (dd, J = 8.4, 2.8 Hz, 1H), 6.67 (d, J = 8.4 Hz, 1H), 5.65 (s, 1H), 5.24 (brs, 1H), 3.58 (brs, 2H), 2.86 (d, J = 5.2 Hz, 3H), 2.16 (s, 3H)·^{13}C NMR (Chloroform-*d*) δ 171.02, 165.38, 158.28, 144.76, 142.15, 123.73, 123.36, 119.86, 115.65, 28.43, 17.59.HRMS (ESI) calcd. for $C_{12}H_{15}N_4O^+$[M + H]$^+$, 231.1240; found, 231.1234.

Please cite this article in press as: Y. Chen, et al., Integrated bioinformatics, computational and experimental methods to discover novel Raf/extracellular-signal regulated kinase (ERK) dual inhibitors against breast cancer cells, European Journal of Medicinal Chemistry (2016), http://dx.doi.org/10.1016/j.ejmech.2016.11.009

4.2.9. 6-(4-Amino-2-methylphenoxy)-N-methylpyrimidin-4-amine (4c)

Yield: 62%, ^{1}H NMR (Chloroform-*d*) δ 8.24 (s, 1H), 6.84 (d, *J* = 8.4 Hz, 1H), 6.57 (d, *J* = 2.8 Hz, 1H), 6.53 (dd, *J* = 8.4, 2.9 Hz, 1H), 5.61 (d, *J* = 0.8 Hz, 1H), 5.20 (brs, 1H), 3.60 (brs, 2H), 2.86 (d, *J* = 5.2 Hz, 3H), 2.08 (s, 3H)·^{13}C NMR (Chloroform-*d*) δ 170.66, 165.44, 158.38, 144.07, 143.38, 131.46, 122.56, 117.68, 113.67, 28.42, 16.31.HRMS (ESI) calcd. for $C_{12}H_{15}N_4O^+$ [M + H]$^+$, 231.1240; found,231.1237.

4.2.10. 3-Fluoro-4-((6-(piperidin-1-yl)pyrimidin-4-yl)oxy)aniline (4d)

Yield: 59%, ^{1}H NMR (Chloroform-*d*) δ 8.27 (d, *J* = 0.8 Hz, 1H), 6.95 (t, *J* = 8.8 Hz, 1H), 6.48 (dd, *J* = 12.0, 2.8 Hz, 1H), 6.43 (ddd, *J* = 8.8, 2.8, 1.2 Hz, 1H), 5.96 (d, *J* = 0.8 Hz, 1H), 3.74 (s, 2H), 3.58 (t, *J* = 5.2 Hz, 4H), 1.71–1.59 (m, 6H)·^{13}C NMR (Chloroform-*d*) δ 170.24, 163.88, 157.89, 154.99 (d, *J* = 247 Hz), 145.27 (d, *J* = 10 Hz), 131.74 (d, *J* = 13 Hz), 124.32 (d, *J* = 3 Hz), 110.70 (d, *J* = 3 Hz), 103.48 (d, *J* = 21 Hz), 85.12, 45.32, 25.42, 24.60. HRMS (ESI) calcd. for $C_{15}H_{18}FN_4O^+$ [M + H]$^+$, 289.1459; found, 289.1461.

4.2.11. 3-Fluoro-4-((6-morpholinopyrimidin-4-yl)oxy)aniline (4e)

Yield: 44%, ^{1}H NMR (Chloroform-*d*) δ 8.30 (s, 1H), 6.95 (t, *J* = 8.8 Hz, 1H), 6.49 (dd, *J* = 12.0, 2.8 Hz, 1H), 6.43 (ddd, *J* = 8.8, 2.8, 1.2 Hz, 1H), 5.97 (s, 1H), 3.79–3.76 (m, 4H), 3.74 (s, 2H), 3.60–3.58 (m, 4H)·^{13}C NMR (Chloroform-*d*) δ 170.33, 164.39, 157.87, 154.95 (d, *J* = 247 Hz), 145.40 (d, *J* = 10 Hz), 131.60 (d, *J* = 13 Hz), 124.27 (d, *J* = 3 Hz), 110.69 (d, *J* = 3 Hz), 103.47 (d, *J* = 22 Hz), 85.58, 66.46, 44.41. HRMS (ESI) calcd. for $C_{14}H_{16}FN_4O_2^+$[M + H]$^+$, 291.1252; found, 291.1253.

4.2.12. 2-Methyl-4-((6-morpholinopyrimidin-4-yl)oxy)aniline (4f)

Yield: 51%, ^{1}H NMR (Chloroform-*d*) δ 8.32 (s, 1H), 6.83 (d, *J* = 2.8 Hz, 1H), 6.79 (dd, *J* = 8.4, 2.8 Hz, 1H), 6.67 (d, *J* = 8.4 Hz, 1H), 5.84 (s, 1H), 3.76 (dd, *J* = 5.6, 4.0 Hz, 4H), 3.59 (s, 2H), 3.55 (dd, *J* = 5.6, 4.0 Hz, 4H), 2.16 (s, 3H)·^{13}C NMR (Chloroform-*d*) δ 170.31, 163.37, 157.05, 143.69, 141.14, 122.70, 122.30, 118.80, 114.62, 84.72, 65.42, 43.36, 16.58.HRMS (ESI) calcd. for $C_{15}H_{19}N_4O_2^+$[M + H]$^+$, 287.1503; found, 287.1505.

4.2.13. 3-Methyl-4-((6-(piperidin-1-yl)pyrimidin-4-yl)oxy)aniline (4g)

Yield: 39%, ^{1}H NMR (Chloroform-*d*) δ 8.29 (s, 1H), 6.83 (d, *J* = 8.4 Hz, 1H), 6.57 (d, *J* = 2.8 Hz, 1H), 6.53 (dd, *J* = 8.4, 2.8 Hz, 1H), 5.80 (s, 1H), 3.59 (s, 2H), 3.54 (t, *J* = 5.2 Hz, 4H), 2.08 (s, 3H), 1.68–1.57 (m, 6H)·^{13}C NMR (Chloroform-*d*) δ 169.85, 162.95, 157.16, 142.89, 142.49, 130.44, 121.54, 116.67, 112.66, 83.66, 44.23, 24.38, 23.56, 15.34.HRMS (ESI) calcd. for $C_{16}H_{21}N_4O^+$ [M + H]$^+$, 285.1710; found, 285.1711.

4.2.14. 3-Methyl-4-((6-morpholinopyrimidin-4-yl)oxy)aniline (4 h)

Yield: 55%, ^{1}H NMR (Chloroform-*d*) δ 8.32 (s, 1H), 6.83 (d, *J* = 8.4 Hz, 1H), 6.58 (d, *J* = 2.8 Hz, 1H), 6.54 (dd, *J* = 8.4, 2.8 Hz, 1H), 5.81 (s, 1H), 3.78–3.75 (m, 4H), 3.59 (s, 2H), 3.55 (t, *J* = 4.8 Hz, 4H), 2.08 (s, 3H)·^{13}C NMR (Chloroform-*d*) δ 169.95, 163.43, 157.14, 143.05, 142.31, 130.39, 121.50, 116.66, 112.66, 84.10, 65.42, 43.34, 15.32.HRMS (ESI) calcd. for $C_{15}H_{19}N_4O_2^+$[M + H]$^+$, 287.1503; found, 287.1504.

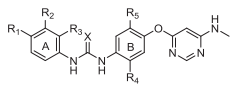

7a-l, 8a-h

Genera procedure for the synthesis of urea derivative compounds 7a-l and 10a-c.

The solution of appropriate aniline (0.5 mmol) and triethylamine (trace) dissolved in toluene (10 mL) was slowly dripped into a stirred solution of triphosgene (59 mg, 0.2 mmol) in toluene (5 mL) at 0 °C by using a constant-pressure dropping funnel. The resulting mixture was then heated to reflux for 6 h after the aniline was added. The organic solvent was removed under vacuum and the residue was taken up in dichloromethane (10 mL), compound 4a-h (0.5 mmol) was added directly to the solution. The reaction mixture was stirred at room temperature for 6 h. The solvent was removedunder vacuumand then purified by column chromatography over silica gel toafford pure compound 7a-l and 10a-c.

4.2.15. 1-(3-Fluoro-4-((6-(methylamino)pyrimidin-4-yl)oxy) phenyl)-3-(3-(trifluoromethyl)phenyl) urea (7a)

Yield: 78%, m.p.: 194.6–195.3 °C. ^{1}H NMR (DMSO-d_6) δ 9.17 (s, 1H, CON**H**), 9.08 (s, 1H, CON**H**), 8.10 (brs, 1H, Pyrimidine Ar-**H**), 8.01 (s, 1H, phenyl A Ar-**H**), 7.63–7.59 (m, 2H, phenyl A Ar-**H**), 7.53 (t, *J* = 8.0 Hz, 1H, phenyl A Ar-**H**), 7.37–7.32 (m, 2H, phenyl B Ar-**H**), 7.24–7.16(m, 2H, Pyrimidine Ar-**H**, phenyl B Ar-**H**), 5.88 (s, 1H, CH_3N**H**), 2.79 (s, 3H, C**H$_3$**NH)·^{13}C NMR (DMSO-d_6) δ 165.08, 153.75 (d, *J* = 244 Hz), 152.43, 140.34, 137.83 (d, *J* = 10 Hz), 133.96 (d, *J* = 13 Hz), 129.89, 129.34 (q, *J* = 32 Hz), 125.50, 124.16 (d, *J* = 2 Hz), 122.80, 121.91, 118.23, 114.52, 114.18 (d, *J* = 4 Hz), 106.68 (d, *J* = 24 Hz), 27.56. HRMS (ESI) calcd. for $C_{19}H_{16}F_4N_5O_2^+$ [M + H]$^+$,422.1235; found, 422.1249. HPLC purity >99%, Rt = 7.2 min.

4.2.16. 1-(4-bromophenyl)-3-(3-fluoro-4-((6-(methylamino) pyrimidin-4-yl)oxy)phenyl)urea (7b)

Yield: 71%, m.p.: 243.1–244.0 °C. ^{1}H NMR (DMSO-d_6) δ 8.96 (s, 1H, CON**H**), 8.92 (s, 1H, CON**H**), 8.10 (brs, 1H, Pyrimidine Ar-**H**), 7.59 (dd, *J* = 13.2, 2.4 Hz, 1H, phenyl B Ar-**H**), 7.48–7.42 (m, 4H, phenyl A Ar-**H**), 7.35 (q, *J* = 4.8 Hz, 1H, phenyl B Ar-**H**), 7.23–7.13 (m, 2H, Pyrimidine Ar-**H**, phenyl B Ar-**H**), 5.88 (s, 1H, CH_3N**H**), 2.78 (s, 3H, C**H$_3$**NH)·^{13}C NMR (DMSO-d_6) δ 164.32, 156.91, 153.67 (d, *J* = 244 Hz), 152.32, 138.89, 138.20 (d, *J* = 10 Hz), 133.59 (d, *J* = 13 Hz), 131.50, 124.11, 120.16, 114.34, 113.38, 106.44 (d, *J* = 24 Hz), 27.65. HRMS (ESI) calcd. for $C_{18}H_{16}BrFN_5O_2^+$ [M'+'H]$^+$, 432.0466; found, 432.0464. HPLC purity >99%, Rt = 6.7 min.

4.2.17. 1-(3-Fluoro-4-((6-(methylamino)pyrimidin-4-yl)oxy) phenyl)-3-(4-methoxyphenyl)urea (7c)

Yield: 77%, m.p.: 226.5–227.4 °C. ^{1}H NMR (DMSO-d_6) δ 8.82 (s, 1H, CON**H**), 8.55 (s, 1H, CON**H**), 8.10 (brs, 1H, Pyrimidine Ar-**H**), 7.59 (dd, *J* = 13.2, 2.4 Hz, 1H, phenyl B Ar-**H**), 7.37–7.32 (m, 3H, phenyl A Ar-**H**), 7.19 (t, *J* = 8.8 Hz, 1H, phenyl B Ar-**H**), 7.12 (dd, *J* = 9.2, 2.4 Hz, 1H, phenyl A Ar-**H**), 6.88 (d, *J* = 8.8 Hz, 2H, phenyl B Ar-**H**), 5.87 (s, 1H, CH_3N**H**), 3.72 (s, 3H, C**H$_3$**O), 2.78 (s, 3H, C**H$_3$**NH)·^{13}C NMR (DMSO-d_6) δ 165.13, 157.73, 154.97 (d, *J* = 244 Hz), 154.58, 152.58, 138.39 (d, *J* = 10 Hz), 133.51 (d, *J* = 13 Hz), 132.37, 124.08, 120.20, 114.10 (d, *J* = 3 Hz), 113.95, 106.26 (d, *J* = 24 Hz), 55.12, 27.45. HRMS (ESI) calcd. for $C_{19}H_{19}FN_5O_3^+$[M + H]$^+$, 384.1466; found, 384.1462. HPLC purity >98%, Rt = 6.4 min.

4.2.18. 1-(3-Fluoro-4-((6-(methylamino)pyrimidin-4-yl)oxy) phenyl)-3-(p-tolyl)urea (7d)

Yield: 69%, m.p.: 234.2–236.1 °C. ^{1}H NMR (DMSO-d_6) δ 8.91 (s, 1H, CON**H**), 8.68 (s, 1H, CON**H**), 8.11 (brs, 1H, Pyrimidine Ar-**H**), 7.60 (dd, *J* = 13.2, 2.4 Hz, 1H, phenyl B Ar-**H**), 7.40 (s, 1H, phenyl A Ar-**H**), 7.34 (d, *J* = 8.4 Hz, 2H, phenyl A Ar-**H**), 7.20 (t, *J* = 8.8 Hz, 1H, phenyl A Ar-**H**), 7.14–7.08 (m, 3H, Pyrimidine Ar-**H**, phenyl B Ar-**H**), 5.88 (s, 1H, CH_3N**H**), 2.79 (s, 3H, C**H$_3$**NH), 2.25 (s, 3H, C**H$_3$**)·^{13}C NMR (DMSO-d_6) δ 164.74, 157.38, 154.94 (d, *J* = 245 Hz), 152.46, 138.41 (d,

Please cite this article in press as: Y. Chen, et al., Integrated bioinformatics, computational and experimental methods to discover novel Raf/extracellular-signal regulated kinase (ERK) dual inhibitors against breast cancer cells, European Journal of Medicinal Chemistry (2016), http://dx.doi.org/10.1016/j.ejmech.2016.11.009

J = 10 Hz), 136.82, 133.47 (d, J = 13 Hz), 130.84, 129.15, 124.08, 118.38, 114.13, 106.26 (d, J = 23 Hz), 27.55, 20.30. HRMS (ESI) calcd. for $C_{19}H_{19}FN_5O_2^+$[M + H]$^+$, 368.1517; found, 368.1523. HPLC purity >98%, Rt = 5.4 min.

4.2.19. 1-(4-Chloro-3-(trifluoromethyl)phenyl)-3-(3-fluoro-4-((6-(methylamino)pyrimidin-4-yl)oxy)phenyl)urea (7e)

Yield: 70%, m.p.: 220.1–221.0 °C. ^{1}H NMR (DMSO-d_6) δ 9.90 (s, 1H, CONH), 9.74 (s, 1H, CONH), 9.04(brs, 1H, phenyl A Ar-H), 8.35 (brs, 1H, phenyl A Ar-H), 8.11 (s, 1H, Pyrimidine Ar-H), 7.68–7.62 (m, 3H, phenyl A Ar-H,, phenyl B Ar-H), 7.30 (t, J = 8.8 Hz, 1H, phenyl B Ar-H), 7.20 (d, J = 9.2, 2.4 Hz, 1H, Pyrimidine Ar-H), 6.07 (brs, 1H, CH_3NH), 2.87 (s, 3H, C$\mathbf{H_3}$NH)·^{13}C NMR (DMSO-d_6) δ 161.24, 154.61 (d, J = 246 Hz), 153.92, 152.42, 139.13, 138.63 (d, J = 9 Hz), 133.08 (d, J = 12 Hz), 132.04, 126.71 (q, J = 31 Hz), 124.09, 123.97, 122.80, 122.36, 121.38, 116.44 (d, J = 6 Hz), 114.50, 106.49 (d, J = 23 Hz), 28.23. HRMS (ESI) calcd. for $C_{19}H_{15}ClF_4N_5O_2^+$ [M + H]$^+$, 456.0845; found, 456.0851.HPLC purity >98%, Rt = 9.8 min.

4.2.20. 1-(2,4-dichlorophenyl)-3-(3-fluoro-4-((6-(methylamino) pyrimidin-4-yl)oxy)phenyl)urea (7f)

Yield: 66%, m.p.: 231.1–232.6 °C. ^{1}H NMR (DMSO-d_6) δ 9.69 (s, 1H, CONH), 8.47 (s, 1H, CONH), 8.19 (d, J = 9.2 Hz, 1H, phenyl A Ar–H), 8.11 (brs, 1H, Pyrimidine Ar–H), 7.65–7.60 (m, 2H, phenyl A Ar–H), 7.42–7.38 (m, 2H, phenyl B Ar–H), 7.23 (t, J = 8.8 Hz, 1H, Pyrimidine Ar–H), 7.15–7.12 (m, 1H, phenyl B Ar–H), 5.89 (s, 1H, CH_3NH), 2.79 (s, 3H, C$\mathbf{H_3}$NH).^{13}C NMR (DMSO-d_6) δ 164.93, 157.57, 153.78 (d, J = 244 Hz), 151.92, 137.69 (d, J = 10 Hz), 134.94, 134.03 (d, J = 13 Hz), 128.56, 127.63, 126.35, 124.29, 122.85, 122.25, 114.34, 106.50 (d, J = 24 Hz), 27.52. HRMS (ESI) calcd. for $C_{18}H_{15}Cl_2FN_5O_2^+$[M + H]$^+$, 422.0581; found, 422.0581. HPLC purity >98%, Rt = 6.3 min.

4.2.21. 1-(2-Methyl-4-((6-(methylamino)pyrimidin-4-yl)oxy) phenyl)-3-(3-(trifluoromethyl)phenyl) urea (7g)

Yield: 72%, m.p.: 190.2–192.3 °C. ^{1}H NMR (DMSO-d_6) δ 9.34 (s, 1H, CONH), 8.13 (s, 1H, CONH), 8.07–8.04 (m, 2H, Pyrimidine Ar–H, phenyl A Ar–H), 7.76 (d, J = 8.8 Hz, 1H, phenyl A Ar–H), 7.55 (dt, J = 15.6, 8.4 Hz, 2H, phenyl B Ar–H), 7.31 (d, J = 7.6 Hz, 1H, phenyl A Ar–H), 7.28 (q, J = 4.8 Hz, 1H, phenyl A Ar–H), 7.00 (d, J = 2.8 Hz, 1H, phenyl B Ar–H), 6.94 (dd, J = 8.8, 2.8 Hz, 1H, Pyrimidine Ar–H), 5.75 (s, 1H, CH_3NH), 2.77 (s, 3H, C$\mathbf{H_3}$NH), 2.25 (s, 3H, C$\mathbf{H_3}$).^{13}C NMR (DMSO-d_6) δ 163.62, 155.61, 152.81, 147.45, 140.79, 134.70, 130.45, 129.89, 129.50 (q, J = 32 Hz), 125.54, 122.89, 122.82, 121.38, 118.86, 117.81, 113.70 (d, J = 4 Hz), 27.77, 17.99. HRMS (ESI) calcd. for $C_{20}H_{19}F_3N_5O_2^+$ [M + H]$^+$, 418.1485; found, 418.1493. HPLC purity >98%, Rt = 6.7 min.

4.2.22. 1-(4-Chloro-3-(trifluoromethyl)phenyl)-3-(2-methyl-4-((6-(methylamino)pyrimidin-4-yl)oxy)phenyl)urea (7h)

Yield: 68%, m.p.: 202.2–203.8 °C. ^{1}H NMR (DMSO-d_6) δ 9.45 (s, 1H, CONH), 8.12 (s, 3H, CONH,, Pyrimidine Ar–H, phenyl A Ar–H), 7.72 (d, J = 8.8 Hz, 1H, phenyl A Ar–H), 7.66–7.60 (m, 2H, phenyl B Ar–H), 7.29 (q, J = 4.8 Hz, 1H, phenyl A Ar–H), 7.01 (d, J = 2.8 Hz, 1H, phenyl B Ar–H), 6.94 (dd, J = 8.8, 2.8 Hz, 1H, Pyrimidine Ar–H), 5.75 (s, 1H, CH_3NH), 2.77 (s, 3H, C$\mathbf{H_3}$NH), 2.24 (s, 3H, C$\mathbf{H_3}$).^{13}C NMR (DMSO-d_6) δ 165.17, 157.93, 152.65, 148.51, 139.47, 133.76, 131.99, 130.85, 126.69 (q, J = 31 Hz), 124.14, 123.46, 123.01, 122.70, 122.06, 121.42, 119.07, 116.46 (d, J = 6 Hz), 27.41, 17.75. HRMS (ESI) calcd. for $C_{20}H_{18}ClF_3N_5O_2^+$[M + H]$^+$, 452.1096; found, 452.1104. HPLC purity >99%, Rt = 5.5 min.

4.2.23. 1-(2,4-dichlorophenyl)-3-(2-methyl-4-((6-(methylamino) pyrimidin-4-yl)oxy)phenyl)urea (7i)

Yield: 65%, m.p.: 220.4–223.4 °C. ^{1}H NMR (DMSO-d_6) δ 8.74 (d, J = 6.0 Hz, 2H, CONH), 8.19 (d, J = 9.2 Hz, 1H, phenyl A Ar–H), 8.15 (brs, 1H, Pyrimidine Ar–H), 7.73 (d, J = 8.8 Hz, 1H, phenyl A Ar–H), 7.63 (d, J = 2.4 Hz, 1H, phenyl A Ar–H), 7.38 (dd, J = 9.2, 2.8 Hz, 2H, phenyl B Ar–H), 7.01 (d, J = 2.8 Hz, 1H, phenyl B Ar–H), 6.94 (dd, J = 8.8, 2.8 Hz, 1H, Pyrimidine Ar–H), 5.76 (s, 1H, CH_3NH), 2.77 (s, 3H, C$\mathbf{H_3}$NH), 2.27 (s, 3H, C$\mathbf{H_3}$).^{13}C NMR (DMSO-d_6) δ 164.81, 157.56, 152.45, 148.26, 135.39, 133.92, 130.70, 128.52, 127.53, 125.97, 123.50, 122.99, 122.62, 122.39, 118.99, 27.49, 17.99. HRMS (ESI) calcd. for $C_{19}H_{18}Cl_2N_5O_2^+$ [M + H]$^+$, 418.0832; found, 418.0837. HPLC purity >99%,Rt = 5.5 min.

4.2.24. 1-(4-chlorophenyl)-3-(2-methyl-4-((6-(methylamino) pyrimidin-4-yl)oxy)phenyl)urea (7j)

Yield: 69%, m.p.: 236.6–239.4 °C. ^{1}H NMR (DMSO-d_6) δ 9.75 (s, 1H, CONH), 8.42 (s, 2H, CONH), 8.26 (brs, 1H, Pyrimidine Ar-H), 7.89 (d, J = 8.8 Hz, 1H, phenyl B Ar-H), 7.53 (d, J = 8.8 Hz, 2H, phenyl A Ar-H), 7.33 (d, J = 8.8 Hz, 2H, phenyl A Ar-H), 7.07 (s, 1H, phenyl B Ar-H), 7.03 (d,, J = 8.0 Hz, 1H, phenyl B Ar-H), 5.81 (s, 1H, CH_3NH), 2.85 (s, 3H, C$\mathbf{H_3}$NH), 2.29 (s, 3H, C$\mathbf{H_3}$)·^{13}C NMR (DMSO-d_6) δ 162.80, 154.38, 152.72, 146.83, 138.96, 135.31, 130.15, 128.59, 125.03, 122.70, 122.48, 119.29, 118.75, 27.97, 18.11. HRMS (ESI) calcd. for $C_{19}H_{19}ClN_5O_2^+$ [M + H]$^+$, 384.1222; found, 384.1219. HPLC purity >96%, Rt = 4.4 min.

4.2.25. 1-(4-methoxyphenyl)-3-(2-methyl-4-((6-(methylamino) pyrimidin-4-yl)oxy)phenyl)urea (7k)

Yield: 66%, m.p.: 237.9–238.6 °C. ^{1}H NMR (DMSO-d_6) δ 8.86 (s, 1H, CONH), 8.15 (brs, 1H, Pyrimidine Ar-H), 7.90 (s, 1H, CONH), 7.81 (d, J = 8.8 Hz, 1H, phenyl A Ar-H), 7.39–7.34(m, 3H, phenyl A Ar-H, phenyl B Ar-H), 6.98 (d, J = 2.8 Hz, 1H, phenyl A Ar-H), 6.92 (dd, J = 8.8, 2.8 Hz, 1H, phenyl A Ar-H), 6.89–6.85 (m, 2H, phenyl B Ar-H, Pyrimidine Ar-H), 5.73 (s, 1H, CH_3NH), 3.72 (s, 3H, C$\mathbf{H_3}$O), 2.77 (s, 3H, C$\mathbf{H_3}$NH), 2.24 (s, 3H, C$\mathbf{H_3}$)·^{13}C NMR (DMSO-d_6) δ 164.85, 157.59, 154.29, 152.89, 147.55, 134.76, 132.89, 129.55, 122.90, 122.31, 119.66, 118.96, 113.99, 55.12, 27.47, 17.86. HRMS (ESI) calcd. for $C_{20}H_{22}N_5O_3^+$ [M + H]$^+$, 380.1717; found, 380.1725.HPLC purity >97%, Rt = 5.3 min.

4.2.26. 1-(3-bromophenyl)-3-(2-methyl-4-((6-(methylamino) pyrimidin-4-yl)oxy)phenyl)urea (7l)

Yield: 67%, m.p.: 205.4–207.4 °C. ^{1}H NMR (DMSO-d_6) δ 9.55 (s, 1H, CONH), 8.28 (s, 2H, CONH, Pyrimidine Ar-H), 7.89 (s, 1H, phenyl A Ar-H), 7.82 (d, J = 8.8 Hz, 2H, phenyl A Ar-H), 7.32–7.30 (m, 1H, phenyl A Ar-H), 7.24 (t, J = 8.0 Hz, 1H, phenyl B Ar-H), 7.14 (dt, J = 8.0, 1.2 Hz, 1H, phenyl B Ar-H), 7.04 (s, 1H, phenyl B Ar-H), 6.98 (d, J = 8.8, 2.8 Hz, 1H, Pyrimidine Ar-H), 5.78 (d, J = 6.8 Hz, 1H, CH_3NH), 2.81 (s, 3H, C$\mathbf{H_3}$NH), 2.27 (s, 3H, C$\mathbf{H_3}$)·^{13}C NMR (DMSO-d_6) δ 163.93, 156.09, 152.64, 147.52, 141.60, 134.66, 130.69, 130.30, 124.11, 122.84, 122.76, 121.73, 120.06, 118.89, 116.66, 27.71, 17.97. HRMS (ESI) calcd. for $C_{19}H_{19}BrN_5O_2^+$ [M + H]$^+$, 428.0717; found, 428.0717. HPLC purity >97%, Rt = 4.6 min.

Genera procedure for the synthesis of thiourea derivative compounds 8a-h.

The solution of appropriate aniline (2 mmol) was stirred in 10 mL of carbon disulphide at room temperature. To the mixture, triethylamine (606 mg, 6 mmol) was added. After 3 h, the resulting mixture was cooled to 0 °C. A solution of di-*tert*-butyl dicarbonate(436 mg, 2 mmol) in EtOH (5 mL) was added into the resulting mixture, followed by adding 4-dimethylaminopyridine (24 mg, 0.2 mmol).The resulting mixture was stirred at room temperature for another 1 h. The organic solvent was removed-under vacuumand theresidue was taken up inacetonitrile (10 mL). Compound 4a-c (2 mmol) was added directly to the solution. The reaction mixturewas stirred at room temperature for 12 h. The solvent was removedunder vacuumand then purified by column

Please cite this article in press as: Y. Chen, et al., Integrated bioinformatics, computational and experimental methods to discover novel Raf/extracellular-signal regulated kinase (ERK) dual inhibitors against breast cancer cells, European Journal of Medicinal Chemistry (2016), http://dx.doi.org/10.1016/j.ejmech.2016.11.009

chromatography over silica gel to afford compound 8a-h.

4.2.27. 1-(3-Fluoro-4-((6-(methylamino)pyrimidin-4-yl)oxy) phenyl)-3-phenylthiourea (8a)

Yield: 53%, m.p.: 171.4–172.1 °C. ^{1}H NMR (DMSO-d_6) δ 9.94 (d, J = 10.0 Hz, 2H, CON**H**), 8.10 (brs, 1H, Pyrimidine Ar-**H**), 7.65 (d, J = 10.0 Hz, 1H, phenyl B Ar-**H**), 7.49 (d, 2H, phenyl A Ar-**H**), 7.41–7.33 (m, 3H, phenyl A Ar-**H**), 7.29–7.22 (m, 2H, phenyl B Ar-**H**), 7.17–7.13 (m, 1H, Pyrimidine Ar-**H**), 5.93 (s, 1H, CH_3N**H**), 2.79 (s, 3H, C**H$_3$**NH).^{13}CNMR (100 MHz, DMSO-d_6) δ 179.55, 165.22, 157.71, 153.23 (d, J = 245 Hz), 139.17, 137.74 (d, J = 10 Hz), 135.91 (d, J = 13 Hz), 128.50, 124.63, 123.72, 123.66, 119.66 (d, J = 3 Hz), 111.76 (d, J = 22 Hz), 27.51. HRMS (ESI) calcd. for $C_{18}H_{17}FN_5OS^+$ $[M + H]^+$, 370.1132; found, 370.1142.HPLC purity >99%, Rt = 13.1min.

4.2.28. 1-(2-Methyl-4-((6-(methylamino)pyrimidin-4-yl)oxy) phenyl)-3-phenylthiourea (8b)

Yield: 50%, m.p.: 145.7–146.5 °C. ^{1}H NMR (DMSO-d_6) δ 9.71 (s, 1H, CON**H**), 9.31 (s, 1H, CON**H**), 8.14 (brs, 1H, Pyrimidine Ar-**H**), 7.50–7.48 (m, 2H, phenyl A Ar-**H**), 7.36–7.31 (m, 3H, phenyl A Ar-**H**), 7.28 (d, J = 8.4 Hz, 1H, phenyl B Ar-**H**), 7.15–7.11 (m, 1H, phenyl B Ar-**H**), 7.03 (d, J = 2.8 Hz, 1H, phenyl B Ar-**H**), 6.95 (dd, J = 8.4, 2.8 Hz, 1H, Pyrimidine Ar-**H**), 5.82 (s, 1H, CH_3N**H**), 2.77 (s, 3H, C**H$_3$**NH), 2.24 (s, 3H, C**H$_3$**)· ^{13}C NMR (DMSO-d_6) δ 180.50, 165.15, 157.85, 150.97, 139.44, 136.62, 134.60, 129.20, 128.41, 124.41, 123.76, 122.84, 118.93, 27.48, 17.90. HRMS (ESI) calcd. for $C_{19}H_{20}N_5OS^+$ $[M + H]^+$, 366.1383; found, 366.1389.HPLC purity >99%, Rt = 10.2 min.

4.2.29. 1-(4-bromophenyl)-3-(2-methyl-4-((6-(methylamino) pyrimidin-4-yl)oxy)phenyl)thiourea (8c)

Yield: 48%, m.p.: 182.4–182.7 °C. ^{1}H NMR (DMSO-d_6) δ 9.76 (s, 1H, CON**H**), 9.42 (s, 1H, CON**H**), 8.13 (brs, 1H, Pyrimidine Ar-**H**), 7.52–7.47 (m, 4H, phenyl A Ar-**H**), 7.34 (q, J = 4.7 Hz, 1H, phenyl B Ar-**H**), 7.26 (d, J = 8.4 Hz, 1H, phenyl B Ar-**H**), 7.03 (d, J = 2.8 Hz, 1H, phenyl B Ar-**H**), 6.95 (dd, J = 8.4, 2.8 Hz, 1H, Pyrimidine Ar-**H**), 5.83 (s, 1H, CH_3N**H**), 2.78 (s, 3H, C**H$_3$**NH), 2.23 (s, 3H, C**H$_3$**)· ^{13}C NMR (DMSO-d_6) δ 180.53, 165.14, 157.87, 151.08, 138.97, 136.63, 134.38, 131.13, 129.15, 125.70, 122.88, 118.99, 116.35, 27.47, 17.87. HRMS (ESI) calcd. for $C_{19}H_{19}BrN_5OS^+$ $[M + H]^+$, 444.0488; found, 444.0496.HPLC purity >99%, Rt = 9.5 min.

4.2.30. 1-(3-Methyl-4-((6-(methylamino)pyrimidin-4-yl)oxy) phenyl)-3-phenylthiourea (8d)

Yield: 45%, m.p.: 164.6–165.2 °C. ^{1}H NMR (DMSO-d_6) δ 9.78 (s, 1H, CON**H**), 9.74 (s, 1H, CON**H**), 8.11 (brs, 1H, Pyrimidine Ar-**H**), 7.49–7.47 (m, 2H, phenyl B Ar-**H**), 7.39–7.29 (m, 5H, phenyl A Ar-**H**), 7.15–7.11 (m, 1H, phenyl B Ar-**H**), 7.01 (d, J = 8.4 Hz, 1H, Pyrimidine Ar-**H**), 5.76 (s, 1H, CH_3N**H**), 2.77 (s, 3H, C**H$_3$**NH), 2.06 (s, 3H, C**H$_3$**)· ^{13}C NMR (DMSO-d_6) δ 179.64, 165.13, 157.96, 147.74, 139.41, 136.41, 130.14, 128.41, 126.40, 124.41, 123.67, 122.77, 121.90, 27.46, 15.97. HRMS (ESI) calcd. for $C_{19}H_{19}N_5NaOS^+$$[M + Na]^+$, 388.1203; found, 388.1209.HPLC purity >99%, Rt = 4.3 min.

4.2.31. 1-(3-Fluoro-4-((6-(methylamino)pyrimidin-4-yl)oxy) phenyl)-3-(3-(trifluoromethyl)phenyl) thiourea (8e)

Yield: 44%, m.p.: 154.4–155.1 °C. ^{1}H NMR (DMSO-d_6) δ 10.15 (d, J = 4.4 Hz, 2H, CON**H**), 8.10 (brs, 1H, Pyrimidine Ar-**H**), 7.95 (s, 1H, phenyl A Ar-**H**), 7.76 (d, J = 8.4 Hz, 1H, phenyl A Ar-**H**), 7.64–7.56 (m, 2H, phenyl A Ar-**H**), 7.49 (d, J = 7.6 Hz, 1H, phenyl B Ar-**H**), 7.40 (q, J = 4.8 Hz, 1H, Pyrimidine Ar-**H**), 7.27 (d, J = 6.0 Hz, 2H, phenyl B Ar-**H**), 5.94 (s, 1H, CH_3N**H**), 2.79 (s, 3H, C**H$_3$**NH)· ^{13}C NMR (DMSO-d_6) δ 179.83, 165.18, 157.85, 153.34 (d, J = 245 Hz), 140.22, 137.28 (d, J = 10 Hz), 136.28 (d, J = 13 Hz), 129.53, 129.01 (q, J = 32 Hz), 127.46, 125.37, 123.85, 122.66, 120.80, 119.92, 112.02 (d, J = 22 Hz), 27.51. HRMS (ESI) calcd. for $C_{19}H_{15}F_4N_5NaOS^+$ $[M + Na]^+$, 460.0826; found, 460.0832.HPLC purity >99%, Rt = 9.1 min.

4.2.32. 1-(2-Methyl-4-((6-(methylamino)pyrimidin-4-yl)oxy) phenyl)-3-(3-(trifluoromethyl)phenyl) thiourea (8f)

Yield: 41%, m.p.: 128.6–130.3 °C. ^{1}H NMR (DMSO-d_6) δ 9.89 (s, 1H, CON**H**), 9.58 (s, 1H, CON**H**), 8.14 (brs, 1H, Pyrimidine Ar-**H**), 7.97 (s, 1H, phenyl A Ar-**H**), 7.80–7.78 (m, 1H, phenyl A Ar-**H**), 7.56 (t, J = 8.0 Hz, 1H, phenyl A Ar-**H**), 7.46 (d, J = 7.6 Hz, 1H, phenyl A Ar-**H**), 7.34 (q, J = 4.8 Hz, 1H, phenyl B Ar-**H**), 7.29 (d, J = 8.4 Hz, 1H, phenyl B Ar-**H**), 7.05(m, 1H, phenyl B Ar-**H**), 6.97 (dd, J = 8.4, 2.8 Hz, 1H, Pyrimidine Ar-**H**), 5.84 (s, 1H, CH_3N**H**), 2.78 (s, 3H, C**H$_3$**NH), 2.25 (s, 3H, C**H$_3$**)· ^{13}C NMR (DMSO-d_6) δ 180.69, 165.18, 157.85, 151.21, 140.52, 136.66, 134.14, 129.38, 129.14,128.88 (q, J = 32 Hz), 127.38, 125.41, 122.95, 122.70, 120.51, 119.83, 119.09, 27.47, 17.82. HRMS (ESI) calcd. for $C_{20}H_{19}F_3N_5OS^+$ $[M + H]^+$, 434.1257; found, 434.1261.HPLC purity >99%, Rt = 7.5 min.

4.2.33. 1-(4-Chloro-3-(trifluoromethyl)phenyl)-3-(3-fluoro-4-((6-(methylamino)pyrimidin-4-yl)oxy)phenyl)thiourea (8g)

Yield: 49%, m.p.: 157.6–158.9 °C. ^{1}H NMR (DMSO-d_6) δ 10.21 (d, J = 12.0 Hz, 2H, CON**H**), 8.08 (d, J = 2.4 Hz, 2H, Pyrimidine Ar-**H**, phenyl A Ar-**H**), 7.80 (dd, J = 8.8, 2.4 Hz, 1H, phenyl A Ar-**H**), 7.69 (d, J = 8.8 Hz, 1H, phenyl A Ar-**H**), 7.60 (dd, J = 12.0, 2.4 Hz, 1H, phenyl B Ar-**H**), 7.40 (q, J = 4.8 Hz, 1H, phenyl B Ar-**H**), 7.31–7.24 (m, 2H, phenyl B Ar-**H**, Pyrimidine Ar-**H**), 5.95 (s, 1H, CH_3N**H**), 2.79 (s, 3H, C**H$_3$**NH)· ^{13}C NMR (DMSO-d_6) δ 179.80, 165.15, 157.72, 153.37 (d, J = 245 Hz), 138.97, 137.09 (d, J = 9 Hz), 136.43 (d, J = 13 Hz), 131.55, 128.65, 126.23 (q, J = 31 Hz), 125.35, 124.01, 123.91, 122.56 (d, J = 6 Hz), 121.30, 120.01 (d, J = 3 Hz), 112.14 (d, J = 22 Hz), 27.47. HRMS (ESI) calcd. for $C_{19}H_{14}ClF_4N_5NaOS^+$ $[M + Na]^+$, 494.0436; found, 494.0440.HPLC purity >99%,Rt = 13.4 min.

4.2.34. 1-(4-Chloro-3-(trifluoromethyl)phenyl)-3-(2-methyl-4-((6-(methylamino)pyrimidin-4-yl)oxy)phenyl)thiourea (8h)

Yield: 43%, m.p.: 132.4–134.1 °C. ^{1}H NMR (DMSO-d_6) δ 9.95 (s, 1H, CON**H**), 9.66 (s, 1H, CON**H**), 8.13 (s, 1H, Pyrimidine Ar-**H**), 8.10 (d, J = 2.8 Hz, 1H, phenyl A Ar-**H**), 7.83 (dd, J = 8.8, 2.8 Hz, 1H, phenyl A Ar-**H**), 7.66 (d, J = 8.8 Hz, 1H, phenyl A Ar-**H**), 7.35 (q, J = 4.8 Hz, 1H, phenyl B Ar-**H**), 7.27 (d, J = 8.4 Hz, 1H, phenyl B Ar-**H**), 7.06 (d, J = 2.8 Hz, 1H, phenyl B Ar-**H**), 6.97 (dd, J = 8.4, 2.8 Hz, 1H, Pyrimidine Ar-**H**), 5.84 (s, 1H, CH_3N**H**), 2.78 (s, 3H, C**H$_3$**NH), 2.24 (s, 3H, C**H$_3$**)· ^{13}C NMR (DMSO-d_6) δ 180.63, 165.10, 157.91, 151.30, 139.27, 136.67, 134.00, 131.81, 131.41, 129.12, 128.52, 126.11 (q, J = 31 Hz), 125.01, 124.05, 122.98, 122.39, 121.33, 119.14, 26.31, 17.80. HRMS (ESI) calcd. for $C_{20}H_{18}ClF_3N_5OS^+$ $[M + H]^+$, 468.0867; found, 468.0862.HPLC purity >99%, Rt = 7.7 min.

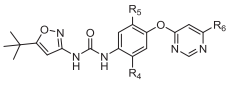

Genera procedure for the synthesis of thiourea derivative compounds 9a-g.

5-(*tert*-butyl)-3-isocyanatoisoxazole (166 mg, 1 mmol) was stirred in 10 mL of dichloromethane at room temperature. To the mixture, compound 4a-b, 4d-h (1 mmol) was added. The resulting mixture was stirred at room temperature for 1 h. The solvent was removed under vacuum and then purified by column chromatography over silica gel to afford compound 9a-g.

4.2.35. 1-(5-(tert-butyl)isoxazol-3-yl)-3-(3-fluoro-4-((6-(methylamino)pyrimidin-4-yl)oxy)phenyl) urea (9a)

Yield: 56%, m.p.: 208.6–209.2 °C. ^{1}H NMR (DMSO-d_6) δ 9.60 (s, 1H, CON**H**), 9.02 (s, 1H, CON**H**), 8.09 (brs, 1H, Pyrimidine Ar-**H**), 7.60

(dd, J = 12.8, 2.4 Hz, 1H, phenyl Ar-**H**), 7.35 (q, J = 4.8 Hz, 1H, phenyl Ar-**H**), 7.22 (t, J = 8.8 Hz, 1H, phenyl Ar-**H**), 7.15 (dd, J = 9.2, 2.4 Hz, 1H, Pyrimidine Ar-**H**), 6.50 (s, 1H, Isoxazole Ar-**H**), 5.88 (s, 1H, CH_3N**H**), 2.78 (s, 3H, C**H$_3$**NH), 1.29 (s, 9H, C**H$_3$**). ^{13}C NMR (DMSO-d_6) δ 180.23, 165.19, 158.20, 157.80, 153.75 (d, J = 244 Hz), 151.30, 137.31 (d, J = 10 Hz), 134.29 (d, J = 13 Hz), 124.23 (d, J = 2 Hz), 114.66, 106.81 (d, J = 24 Hz), 92.47, 32.44, 28.30, 27.48. HRMS (ESI) calcd. for $C_{19}H_{22}FN_6O_3^+$ [M + H]$^+$, 401.1732; found, 401.1737. HPLC purity>99%, Rt = 11.7 min.

4.2.36. 1-(5-(tert-butyl)isoxazol-3-yl)-3-(3-fluoro-4-((6-(piperidin-1-yl)pyrimidin-4-yl)oxy)phenyl) urea (9b)

Yield: 53%, m.p.: 222.2–223.1 °C. ^{1}H NMR (DMSO-d_6) δ 9.59 (s, 1H, CON**H**), 9.02 (s, 1H, CON**H**), 8.13 (d, J = 0.8 Hz, 1H, Pyrimidine Ar-**H**), 7.59 (dd, J = 12.8, 2.4 Hz, 1H, phenyl Ar-**H**), 7.21 (t, J = 8.8 Hz, 1H, phenyl Ar-**H**), 7.16–7.13 (m, 1H, phenyl Ar-**H**), 6.51 (s, 1H, Isoxazole Ar-**H**), 6.34 (d, J = 0.8 Hz, 1H, Pyrimidine Ar-**H**), 3.61 (t, J = 5.2 Hz, 4H, Piperidine C**H$_2$**), 1.63 (q, J = 6.4 Hz, 2H, Piperidine C**H$_2$**), 1.55–1.52 (m, 4H, Piperidine C**H$_2$**), 1.30 (s, 9H, C**H$_3$**). ^{13}C NMR (DMSO-d_6) δ 180.23, 169.19, 163.37, 158.20, 157.31, 153.77 (d, J = 244.2 Hz), 151.31, 137.21 (d, J = 10.0 Hz), 134.37 (d, J = 12.7 Hz), 124.19, 114.57 (d, J = 3.0 Hz), 106.76 (d, J = 23.5 Hz), 92.46, 85.13, 44.70, 32.44, 28.31, 25.01, 24.09. HRMS (ESI) calcd. for $C_{23}H_{28}FN_6O_3^+$ [M + H]$^+$, 455.2201; found, 455.2199. HPLC purity >99%, Rt = 16.1 min.

4.2.37. 1-(5-(tert-butyl)isoxazol-3-yl)-3-(3-fluoro-4-((6-morpholinopyrimidin-4-yl)oxy)phenyl) urea (9c)

Yield: 59%, m.p.: 219.7–221.2 °C. ^{1}H NMR (DMSO-d_6) δ 9.60 (s, 1H, CON**H**), 9.03 (s, 1H, CON**H**), 8.18 (d, J = 0.8 Hz, 1H, Pyrimidine Ar-**H**), 7.60 (dd, J = 12.8, 2.4 Hz, 1H, phenyl Ar-**H**), 7.22 (t, J = 8.8 Hz, 1H, phenyl Ar-**H**), 7.17–7.14 (m, 1H, phenyl Ar-**H**), 6.50 (s, 1H, Isoxazole Ar-**H**), 6.39 (s, 1H, Pyrimidine Ar-**H**), 3.68–3.66 (m, 4H, Morpholin C**H$_2$**), 3.59 (q, J = 4.8, 4.0 Hz, 4H, Morpholin C**H$_2$**), 1.30 (s, 9H, C**H$_3$**). ^{13}C NMR (DMSO-d_6) δ 180.24, 169.17, 163.97, 158.19, 157.29, 153.72 (d, J = 244 Hz), 151.30, 137.32 (d, J = 10 Hz), 134.25 (d, J = 13 Hz), 124.17, 114.59 (d, J = 3 Hz), 106.76 (d, J = 24 Hz), 92.47, 85.67, 65.70, 44.04, 32.45, 28.31. HRMS (ESI) calcd. for $C_{22}H_{26}FN_6O_4^+$ [M + H]$^+$, 457.1994; found, 457.1991. HPLC purity >99%, Rt = 8.0 min.

4.2.38. 1-(5-(tert-butyl)isoxazol-3-yl)-3-(2-methyl-4-((6-(methylamino)pyrimidin-4-yl)oxy)phenyl) urea (9d)

Yield: 50%, m.p.: 131.5–134.5 °C. ^{1}H NMR (DMSO-d_6) δ 10.05 (s, 1H, CON**H**), 8.62 (s, 1H, CON**H**), 8.21 (m, 1H, Pyrimidine Ar–**H**), 7.83 (d, J = 8.8 Hz, 1H, phenyl Ar–**H**), 7.60 (s, 1H, phenyl Ar–**H**), 7.02 (d, J = 2.4 Hz, 1H, phenyl Ar–**H**), 6.96 (dd, J = 8.8, 2.8 Hz, 1H, Isoxazole Ar–**H**), 6.47 (s, 1H, Pyrimidine Ar–**H**), 5.78 (s, 1H, CH_3N**H**), 2.79 (s, 3H, C**H$_3$**NH), 2.27 (s, 3H, C**H$_3$**), 1.30 (s, 9H, C**H$_3$**). ^{13}C NMR (DMSO-d_6) δ 180.02, 164.35, 158.45, 156.85, 151.70, 147.93, 134.12, 130.14, 122.94, 122.54, 118.97, 92.35, 32.41, 28.32, 27.59, 17.88. HRMS (ESI) calcd. for $C_{20}H_{25}N_6O_3^+$ [M + H]$^+$, 397.1983; found, 397.1985. HPLC purity >99%, Rt = 6.5 min.

4.2.39. 1-(5-(tert-butyl)isoxazol-3-yl)-3-(2-methyl-4-((6-morpholinopyrimidin-4-yl)oxy)phenyl) urea (9e)

Yield: 51%, m.p.: 205.5–208.5 °C. ^{1}H NMR (DMSO-d_6) δ 9.85 (s, 1H, CON**H**), 8.29 (s, 1H, CON**H**), 8.20 (s, 1H, Pyrimidine Ar–**H**), 7.80 (d, J = 8.8 Hz, 1H, phenyl Ar–**H**), 6.99 (d, J = 2.8 Hz, 1H, phenyl Ar–**H**), 6.92 (dd, J = 8.8, 2.8 Hz, 1H, phenyl Ar–**H**), 6.45 (s, 1H, Isoxazole Ar–**H**), 6.26 (s, 1H, Pyrimidine Ar–**H**), 3.67–3.65 (m, 4H, Morpholin C**H$_2$**), 3.57–3.55 (m, 4H, Morpholin C**H$_2$**), 2.24 (s, 3H, C**H$_3$**), 1.29 (s, 9H, C**H$_3$**). ^{13}C NMR (DMSO-d_6) δ 180.00, 168.38, 163.25, 158.44, 155.75, 151.72, 147.65, 134.27, 130.04, 122.80, 122.38, 118.82, 92.36, 86.00, 65.62, 44.37, 32.41, 28.32, 17.97. HRMS (ESI) calcd. for $C_{23}H_{29}N_6O_4^+$ [M + H]$^+$, 453.2245; found, 453.2239. HPLC purity >99%, Rt = 7.6 min.

4.2.40. 1-(5-(tert-butyl)isoxazol-3-yl)-3-(3-methyl-4-((6-(piperidin-1-yl)pyrimidin-4-yl)oxy)phenyl) urea (9f)

Yield: 55%, m.p.: 223.1–223.7 °C. ^{1}H NMR (DMSO-d_6) δ 9.50 (s, 1H, CON**H**), 8.77 (s, 1H, CON**H**), 8.11 (s, 1H, Pyrimidine Ar–**H**), 7.38 (d, J = 2.4 Hz, 1H, phenyl Ar–**H**), 7.27 (dd, J = 8.8, 2.8 Hz, 1H, phenyl Ar–**H**), 6.96 (d, J = 8.8 Hz, 1H, phenyl Ar–**H**), 6.50 (s, 1H, Isoxazole Ar–**H**), 6.19 (s, 1H, Pyrimidine Ar–**H**), 3.58 (t, J = 5.6 Hz, 4H, Piperidine C**H$_2$**), 2.05 (s, 3H, C**H$_3$**), 1.64–1.60 (m, 2H, Piperidine C**H$_2$**), 1.54–1.51 (m, 4H, Piperidine C**H$_2$**), 1.29 (s, 9H, C**H$_3$**). ^{13}C NMR (DMSO-d_6) δ 180.11, 169.76, 163.41, 158.36, 157.47, 151.33, 146.22, 135.89, 130.55, 122.29, 120.92, 117.25, 92.39, 84.99, 44.61, 32.43, 28.31, 24.99, 24.07, 16.11. HRMS (ESI) calcd. for $C_{24}H_{31}N_6O_3^+$ [M + H]$^+$, 451.2452; found, 451.2446. HPLC purity >98%, Rt = 15.6 min.

4.2.41. 1-(5-(tert-butyl)isoxazol-3-yl)-3-(3-methyl-4-((6-morpholinopyrimidin-4-yl)oxy)phenyl) urea (9g)

Yield: 51%, m.p.: 217.3–218.2 °C. ^{1}H NMR (DMSO-d_6) δ 9.50 (s, 1H, CON**H**), 8.78 (s, 1H, CON**H**), 8.17 (s, 1H, Pyrimidine Ar–**H**), 7.39 (d, J = 2.4 Hz, 1H, phenyl Ar–**H**), 7.28 (dd, J = 8.8, 2.8 Hz, 1H, phenyl Ar–**H**), 6.97 (d, J = 8.8 Hz, 1H, phenyl Ar–**H**), 6.50 (s, 1H, Isoxazole Ar–**H**), 6.24 (s, 1H, Pyrimidine Ar–**H**), 3.67–3.65 (m, 4H, Morpholin C**H$_2$**), 3.57–3.55 (m, 4H, Morpholin C**H$_2$**), 2.06 (s, 3H, C**H$_3$**), 1.30 (s, 9H, C**H$_3$**). ^{13}C NMR (DMSO-d_6) δ 180.12, 169.75, 164.01, 158.36, 157.43, 151.33, 146.11, 135.99, 130.53, 122.29, 120.94, 117.27, 92.39, 85.54, 65.70, 43.97, 32.43, 28.31, 16.10. HRMS (ESI) calcd. for $C_{23}H_{29}N_6O_4^+$ [M+H]$^+$, 453.2245; found, 453.2239. HPLC purity >99%, Rt = 7.7 min.

4.2.42. 1-Cyclopropyl-3-(2-methyl-4-((6-(methylamino)pyrimidin-4-yl)oxy)phenyl)urea (10a)

Yield: 40%, m.p.: 208.6–209.4 °C. ^{1}H NMR (DMSO-d_6) δ 8.11 (brs, 1H, Pyrimidine Ar-**H**), 7.75 (d, J = 8.8 Hz, 1H, phenyl Ar-**H**), 7.54 (s, 1H, CON**H**), 7.25 (q, J = 4.8 Hz, 1H, CON**H**), 6.92 (d, J = 2.8 Hz, 1H, phenyl Ar-**H**), 6.87 (dd, J = 8.8, 2.8 Hz, 1H, phenyl Ar-**H**), 6.69 (d, J = 2.8 Hz, 1H, Pyrimidine Ar-**H**), 5.70 (s, 1H, CH_3N**H**), 2.75 (s, 3H, C**H$_3$**NH), 2.55 (dq, J = 7.2, 3.2 Hz, 1H, Cyclopropyl C**H**), 2.17 (s, 3H, C**H$_3$**), 0.64 (td, J = 6.8, 4.8 Hz, 2H, Cyclopropyl C**H$_2$**), 0.43–0.39 (m, 2H, Cyclopropyl C**H$_2$**). ^{13}C NMR (DMSO-d_6) δ 169.27, 165.05, 158.00, 156.13, 147.37, 135.10, 129.27, 122.80, 122.19, 118.87, 27.40, 22.39, 17.74, 6.36. HRMS (ESI) calcd. for $C_{16}H_{20}N_5O_2^+$ [M + H]$^+$, 314.1612; found, 314.1615. HPLC purity >99%, Rt = 4.5 min.

4.2.43. 1-(2-Methyl-4-((6-(methylamino)pyrimidin-4-yl)oxy)phenyl)-3-(thiazol-2-yl)urea (10b)

Yield: 38%, m.p.: 203.1–205.0 °C. ^{1}H NMR (DMSO-d_6) δ 10.83 (s, 1H, CON**H**), 8.41 (s, 1H, CON**H**), 8.13 (brs, 1H, Pyrimidine Ar-**H**), 7.83 (d, J = 8.8 Hz, 1H, phenyl Ar-**H**), 7.39 (d, J = 3.6 Hz, 1H, Thiazole Ar-**H**), 7.29 (q, J = 4.8 Hz, 1H, phenyl Ar-**H**), 7.12 (d, J = 3.6 Hz, 1H, Thiazole Ar-**H**), 7.02 (d, J = 2.8 Hz, 1H, phenyl Ar-**H**), 6.96 (dd, J = 8.8, 2.8 Hz, 1H, Pyrimidine Ar-**H**), 5.75 (s, 1H, CH_3N**H**), 2.77 (s, 3H, C**H$_3$**NH), 2.25 (s, 3H, C**H$_3$**). ^{13}C NMR (DMSO-d_6) δ 165.09, 159.50, 157.96, 151.70, 148.44, 137.51, 133.44, 130.09, 123.10, 122.51, 119.17, 112.36, 27.43, 17.67. HRMS (ESI) calcd. for $C_{16}H_{17}N_6O_2S^+$ [M + H]$^+$, 357.1128; found, 357.1131. HPLC purity >99%, Rt = 4.3 min.

4.2.44. 1-(benzo[d]thiazol-2-yl)-3-(2-methyl-4-((6-(methylamino)pyrimidin-4-yl)oxy)phenyl)urea (10c)

Yield: 41%, m.p.: 257.9–260.2 °C. ^{1}H NMR (DMSO-d_6) δ 11.23 (brs, 1H, CON**H**), 8.86 (s, 1H, CON**H**), 8.15 (brs, 1H, Pyrimidine Ar-**H**), 7.92 (d, J = 8.0 Hz, 1H, benzothiazole Ar-**H**), 7.83 (d, J = 8.8 Hz, 1H, benzothiazole Ar-**H**), 7.69 (d, J = 8.0 Hz, 1H, benzothiazole Ar-**H**),

Please cite this article in press as: Y. Chen, et al., Integrated bioinformatics, computational and experimental methods to discover novel Raf/extracellular-signal regulated kinase (ERK) dual inhibitors against breast cancer cells, European Journal of Medicinal Chemistry (2016), http://dx.doi.org/10.1016/j.ejmech.2016.11.009

7.42–7.38 (m, 1H, benzothiazole Ar-**H**), 7.31 (q, J = 4.8 Hz, 1H, phenyl Ar-**H**), 7.25 (t, J = 7.2 Hz, 1H, phenyl Ar-**H**), 7.05 (d, J = 2.8 Hz, 1H, phenyl Ar-**H**), 6.99 (dd, J = 8.8, 2.8 Hz, 1H, Pyrimidine Ar-**H**), 5.77 (d, J = 4.8 Hz, 1H, CH_3N**H**), 2.78 (s, 3H, C**H$_3$**NH), 2.31 (s, 3H, C**H$_3$**)· ^{13}C NMR (DMSO-d_6) δ 169.57, 165.62, 159.90, 158.47, 152.29, 149.25, 133.70, 131.83, 131.15, 126.40, 123.65, 123.49, 123.36, 121.94, 120.36, 119.70, 27.92, 18.30. HRMS (ESI) calcd. for $C_{20}H_{19}N_6O_2S^+$ $[M + H]^+$, 407.1285; found, 407.1283. HPLC purity >99%, Rt = 5.4 min.

4.3. Proteomics-based PPI network construction

To build the RAF/MEK/ERK kinase protein–protein interaction (PPI) network, we collected diverse sets of biological evidence from seven online databases. Different PPIs were collected fromthe Database of Interacting Proteins (DIP), Biomolecular Object Network Databank (BOND), Human Protein Reference Database (HPRD), HomoMINT, IntAct, BioGRID and PrePPI. Moreover, we extract the RAF/MEK/ERK subnetwork from the PPI network based on the ITRAQ-based proteomics results.

4.4. Sequence alignment and molecular docking

The sequence alignment between Raf1 and ERK1 were perform by the MODELER module embedded in the Accelrys Discovery Studio 2.5 software packages (BIOVIA, San Diego, CA, USA). The initial coordinates of the X-ray crystal structure of Raf1 (PDB No. 3OMV) and ERK1 (PDB No. 4QTB) were downloaded from the Protein Data Bank (http://www.rcsb.org). Moreover, the ligandfit module embedded in the Accelrys Discovery Studio was used for the generation of binding conformations of compound 9d into Raf1 and ERK1, respectively.

4.5. Kinase inhibition assay and KINOMEscan profiling

Kinase inhibition assays were using KinaseProfiler services provided by Eurofins, and ATP concentrations used are the ATP *Km* of corresponding kinases. The KINOMEScan selectivity profiling data of compound 9d was determined by DiscoveRx Co. Ltd., which was obtained from manufacturer's protocol. The results were shown in Table S1.

4.6. Cell proliferation assay

The cellular proliferation activities of compounds were evaluated in MCF-7 and MD-MBA-231 breast cancer cells. In general, cancer cells seeded in 96-well plates were treated by a series of concentration for 48 h. The mean percentage of cell survival rates were determined from data of three individual experiments, and all the data were expressed as mean value. The cells viability was evaluated by adding the MTT solution (5 mg/ml) to the cells and incubating the cells for 3 h. After that, the MTT solution was removed and the formazan crystals were dissolved in DMSO. The absorbance of the solution was measured at 570 nm. The control group consisted of untreated cells.

4.7. Apoptosis assay

Apoptosis induction assay of compound 9d and BL-EI001 were carried out on MCF-7 cells. The flow cytometric (FCM) analysis was used to confirm the apoptotic induction effect of different micelles. Apoptosis of MCF-7 cells treated with compound 9d, BL-EI001 or saline were determined were gently trypsinized without EDTA and centrifuged at 2000g for five minutes. Then, the harvested cells were washed with 1.0 mL cold PBS by centrifugation at 2000*g* for 5 min and resuspended in 500 μL of binding buffer (1x), containing 5 μL of Annexin V-FITC and 5 μL of propidium iodide (PI), and incubated for 15 min at room temperature. The samples were then measured by FCM (BD FACS Calibur, BD, USA) using the FL1 channel for Annexin V-FITC and the FL2 channel for PI. Both early apoptotic (Annexin V+/PI-) and late apoptotic (Annexin V+/PI+) cells were included in cell apoptosis determinations.

4.8. Western blot analysis

All the primary antibodies were purchased from Cell Signaling Technology or Santa Cruz Biotechnology. After various treatments as indicated in the figure legends, MCF-7 cells were harvested by trypsinization and then washed with cold PBS. The cells were lysed in RIPA buffer (Invitrogen, CA, USA) on ice for 30 min followed by sonication denaturation. Cell lysates were then centrifuged at 13,000 g for 30 min at 4 °C. Supernatant was collected, and protein concentration was determined using a bicinchoninic acid protein assay kit (Thermo, USA). The protein was applied to a 10–15% SDS-polyacrylamide gel, transferred to a nitrocellulose membrane, and then detected by the proper primary and secondary antibodies before visualization by chemiluminescence Kit (Millpore, USA).

Competing interests

The authors declare no competing interests.

Acknowledgements

We are grateful for financial support from the National Natural Science Foundation of China (81273471), China Postdoctoral Science Foundation (No. 2016M602696 and 2016M592679) and the Fundamental Research Funds for the Central Universities and Distinguished Young Scholars of Sichuan University (2015SCU04A13). The sequence alignment, structure superposed results of Raf1 and ERK1, NMR spectrum and KINOMEscan profiling results were supplied as Supporting Information. This material is available free of charge via the Internet.

List of abbreviations

Raf	RAF proto-oncogene serine/threonine-protein kinase
ERK	Extracellular signal–regulated kinases
MEK	Mitogen-activated protein kinase kinase
MAPK	Mitogen-activated protein kinase
iTRAQ	isobaric tags for relative and absolute quantitation
PPI	Protein-protein interaction
FasL	Fas ligand
FADD	Fas-Associated protein with Death Domain
Bax	Bcl-2-associated X protein
Bcl-2	B-cell lymphoma 2
TEA	Triethylamine
DMAP	4-dimethylaminopyridine.

Appendix A. Supplementary data

Supplementary data related to this article can be found at http://dx.doi.org/10.1016/j.ejmech.2016.11.009.

References

[1] R.L. Siegel, K.D. Miller, A. Jemal, Cancer Statistics, Ca-a Cancer J. Clin. 65 (2015) (2015) 5–29.
[2] A. Goldhirsch, E.P. Winer, A.S. Coates, R.D. Gelber, M. Piccart-Gebhart, B. Thurlimann, H.J. Senn, M. Panel, Personalizing the treatment of women with early breast cancer: highlights of the st gallen international expert consensus

on the primary therapy of early breast Cancer 2013, Ann. Oncol. 24 (2013) 2206–2223.
[3] R.D. Lester, M. Jo, W.M. Campana, S.L. Gonias, Erythropoietin promotes MCF-7 breast cancer cell migration by an ERK/mitogen-activated protein kinase-dependent pathway and is primarily responsible for the increase in migration observed in hypoxia, J. Biol. Chem. 280 (2005) 39273–39277.
[4] K.S. Saini, S. Loi, E. de Azambuja, O. Metzger-Filho, M.L. Saini, M. Ignatiadis, J.E. Dancey, M.J. Piccart-Gebhart, Targeting the PI3K/AKT/mTOR and Raf/MEK/ERK pathways in the treatment of breast cancer, Cancer Treat. Rev. 39 (2013) 935–946.
[5] V. Serra, M. Scaltriti, L. Prudkin, P.J.A. Eichhorn, Y.H. Ibrahim, S. Chandarlapaty, B. Markman, O. Rodriguez, M. Guzman, S. Rodriguez, M. Gili, M. Russillo, J.L. Parra, S. Singh, J. Arribas, N. Rosen, J. Baselga, PI3K inhibition results in enhanced HER signaling and acquired ERK dependency in HER2-overexpressing breast cancer, Oncogene 30 (2011) 2547–2557.
[6] L.G. Ahronian, E.M. Sennott, E.M. Van Allen, N. Wagle, E.L. Kwak, J.E. Faris, J.T. Godfrey, K. Nishimura, K.D. Lynch, C.H. Mermel, E.L. Lockerman, A. Kalsy, J.M. Gurski, S. Bahl, K. Anderka, L.M. Green, N.J. Lennon, T.G. Huynh, M. Mino-Kenudson, G. Getz, D. Dias-Santagata, A.J. Iafrate, J.A. Engelman, L.A. Garraway, R.B. Corcoran, Clinical acquired resistance to RAF inhibitor combinations in BRAF-mutant colorectal Cancer through MAPK pathway alterations, Cancer Discov. 5 (2015) 358–367.
[7] M. Endo, H. Yamamoto, N. Setsu, K. Kohashi, Y. Takahashi, T. Ishii, K. Iida, Y. Matsumoto, M. Hakozaki, M. Aoki, H. Iwasaki, Y. Dobashi, K. Nishiyama, Y. Iwamoto, Y. Oda, Prognostic significance of AKT/mTOR and MAPK pathways and antitumor effect of mTOR inhibitor in NF1-related and sporadic malignant peripheral nerve sheath tumors, Clin. Cancer Res. 19 (2013) 450–461.
[8] C. Ingeson-Carlsson, A. Martinez-Monleon, M. Nilsson, Differential effects of MAPK pathway inhibitors on migration and invasiveness of BRAF(V600E) mutant thyroid cancer cells in 2D and 3D culture, Exp. Cell Res. 338 (2015) 127–135.
[9] J. Izrailit, H.K. Berman, A. Datti, J.L. Wrana, M. Reedijk, High throughput kinase inhibitor screens reveal TRB3 and MAPK-ERK/TGF beta pathways as fundamental Notch regulators in breast cancer, Proc. Natl. Acad. Sci. U. S. A. 110 (2013) 1714–1719.
[10] D.C. Kirouac, J.Y. Du, J. Lahdenranta, R. Overland, D. Yarar, V. Paragas, E. Pace, C.F. McDonagh, U.B. Nielsen, M.D. Onsum, Computational modeling of ERBB2-amplified breast Cancer identifies combined ErbB2/3 blockade as superior to the combination of MEK and AKT inhibitors, Sci. Signal. 6 (2013).
[11] H. Zhao, K.M. Cui, F. Nie, L.L. Wang, M.B. Brandl, G.X. Jin, F.H. Li, Y. Mao, Z. Xue, A. Rodriguez, J. Chang, S.T.C. Wong, The effect of mTOR inhibition alone or combined with MEK inhibitors on brain metastasis: an in vivo analysis in triple-negative breast cancer models, Breast Cancer Res. Treat. 131 (2012) 425–436.
[12] B. Liu, L.L. Fu, C. Zhang, L. Zhang, Y.H. Zhang, L. Ouyang, G. He, J. Huang, Computational design, chemical synthesis, and biological evaluation of a novel ERK inhibitor (BL-EI001) with apoptosis-inducing mechanisms in breast cancer, Oncotarget 6 (2015) 6762–6775.
[13] M.W. Zheng, C.H. Zhang, K. Chen, M. Huang, Y.P. Li, W.T. Lin, R.J. Zhang, L. Zhong, R. Xiang, L.L. Li, X.Y. Liu, Y.Q. Wei, S.Y. Yang, Preclinical evaluation of a novel orally available SRC/raf/VEGFR2 inhibitor, SKLB646, in the treatment of triple-negative breast Cancer, Mol. Cancer Ther. 15 (2016) 366–378.
[14] Y.C. Hsiao, M.H. Yeh, Y.J. Chen, J.F. Liu, C.H. Tang, W.C. Huang, Lapatinib increases motility of triple-negative breast cancer cells by decreasing miRNA-7 and inducing Raf-1/MAPK-dependent interleukin-6, Oncotarget 6 (2015) 37965–37978.
[15] J. Gao, X. Liu, F. Yang, T. Liu, Q. Yan, X. Yang, By inhibiting Ras/Raf/ERK and MMP-9, knockdown of EpCAM inhibits breast cancer cell growth and metastasis, Oncotarget 6 (2015) 27187–27198.
[16] K.S. Saini, S. Loi, E. de Azambuja, O. Metzger-Filho, M.L. Saini, M. Ignatiadis, J.E. Dancey, M.J. Piccart-Gebhart, Targeting the PI3K/AKT/mTOR and Raf/MEK/ERK pathways in the treatment of breast cancer, Cancer Treat. Rev. 39 (2013) 935–946.
[17] J.R. Taylor, B.D. Lehmann, W.H. Chappell, S.L. Abrams, L.S. Steelman, J.A. McCubrey, Cooperative effects of Akt-1 and Raf-1 on the induction of cellular senescence in doxorubicin or tamoxifen treated breast cancer cells, Oncotarget 2 (2011) 610–626.
[18] B. Gril, D. Palmieri, Y. Qian, D. Smart, L. Ileva, D.J. Liewehr, S.M. Steinberg, P.S. Steeg, Pazopanib reveals a role for tumor cell B-Raf in the prevention of HER2+ breast cancer brain metastasis, Clin. cancer Res. official J. Am. Assoc. Cancer Res. 17 (2011) 142–153.
[19] B. Escudier, T. Eisen, W.M. Stadler, C. Szczylik, S. Oudard, M. Siebels, S. Negrier, C. Chevreau, E. Solska, A.A. Desai, F. Rolland, T. Demkow, T.E. Hutson, M. Gore, S. Freeman, B. Schwartz, M.H. Shan, R. Simantov, R.M. Bukowski, T.S. Grp, Sorafenib in advanced clear-cell renal-cell carcinoma, N. Engl. J. Med. 356 (2007) 125–134.
[20] S. Wilhelm, C. Carter, M. Lynch, T. Lowinger, J. Dumas, R.A. Smith, B. Schwartz, R. Simantov, S. Kelley, Discovery and development of sorafenib: a multikinase inhibitor for treating cancer, Nat. Rev. Drug Discov. 5 (2006) 835–844.
[21] R.B. Corcoran, H. Ebi, A.B. Turke, E.M. Coffee, M. Nishino, A.P. Cogdill, R.D. Brown, P. Della Pelle, D. Dias-Santagata, K.E. Hung, K.T. Flaherty, A. Piris, J.A. Wargo, J. Settleman, M. Mino-Kenudson, J.A. Engelman, Egfr-mediated reactivation of MAPK signaling contributes to insensitivity of BRAF-mutant colorectal cancers to RAF inhibition with vemurafenib, Cancer Discov. 2 (2012) 227–235.
[22] G.V. Long, U. Trefzer, M.A. Davies, R.F. Kefford, P.A. Ascierto, P.B. Chapman, I. Puzanov, A. Hauschild, C. Robert, A. Algazi, L. Mortier, H. Tawbi, T. Wilhelm, L. Zimmer, J. Switzky, S. Swann, A.M. Martin, M. Guckert, V. Goodman, M. Streit, J.M. Kirkwood, D. Schadendorf, Dabrafenib in patients with Val600Glu or Val600Lys BRAF-mutant melanoma metastatic to the brain (BREAK-MB): a multicentre, open-label, phase 2 trial, Lancet Oncol. 13 (2012) 1087–1095.
[23] Z. Li, K. Jiang, X.F. Zhu, G.B. Lin, F. Song, Y.F. Zhao, Y.J. Piao, J.W. Liu, W. Cheng, X.L. Bi, P. Gong, Z.Q. Song, S.S. Meng, Encorafenib (LGX818), a potent BRAF inhibitor, induces senescence accompanied by autophagy in BRAFV600E melanoma cells, Cancer Lett. 370 (2016) 332–344.
[24] J. James, B. Ruggeri, R.C. Armstrong, M.W. Rowbottom, S. Jones-Bolin, R.N. Gunawardane, P. Dobrzanski, M.F. Gardner, H. Zhao, M.D. Cramer, K. Hunter, R.R. Nepomuceno, M.G. Cheng, D. Gitnick, M. Yazdanian, D.E. Insko, M.A. Ator, J.L. Apuy, R. Faraoni, B.D. Dorsey, M. Williams, S.S. Bhagwat, M.W. Holladay, CEP-32496: a novel orally active BRAF(V600E) inhibitor with selective cellular and in vivo antitumor activity, Mol. Cancer Ther. 11 (2012) 930–941.
[25] M. Martinez-Garcia, U. Banerji, J. Albanell, R. Bahleda, S. Dolly, F. Kraeber-Bodere, F. Rojo, E. Routier, E. Guarin, Z.X. Xu, R. Rueger, J.J.L. Tessier, E. Shochat, S. Blotner, V.M. Naegelen, J.C. Soria, First-in-Human, phase I dose-escalation study of the safety, pharmacokinetics, and pharmacodynamics of RO5126766, a first-in-class dual MEK/RAF inhibitor in patients with solid tumors, Clin. Cancer Res. 18 (2012) 4806–4819.
[26] M. Ohori, M. Takeuchi, R. Maruki, H. Nakajima, H. Miyake, FR180204, a novel and selective inhibitor of extracellular signal-regulated kinase, ameliorates collagen-induced arthritis in mice, Naunyn-Schmiedebergs Archives Pharmacol. 374 (2007) 311–316.
[27] A.M. Miermont, H. Pflicke, H. Guan, H. Chinnasamy, C. Thomas, U. Rudloff, Direct inhibition of ERK1/2 by VTX-11e leads to increased induction of apoptosis in a subset of pancreatic cancer cell lines as compared to MEK1/2 inhibition by selumetinib (AZD6244), Cancer Res. 73 (2013).
[28] C.X. Hu, T. Dadon, V. Chenna, S. Yabuuchi, R. Bannerji, R. Booher, P. Strack, A. Samatar, N. Azad, B.D. Nelkin, A. Maitra, Combined inhibition of cyclin-dependent kinases (Dinaciclib) and AKT (MK-2206) or ERK (SCH772984) dramatically blocks pancreatic tumor growth and metastases in patient-derived orthotopic xenograft models, Mol. Cancer Ther. 12 (2013).
[29] J.R. Infante, F. Janku, A.W. Tolcher, M.R. Patel, R.J. Sullivan, K. Flaherty, R.D. Carvajal, A.M. Varghese, D.J.L. Wong, M. Sznol, J.A. Sosman, A. Wang-Gillam, H.A. Burris, A. Ribas, S.P. Patel, D.J. Welsch, S. Saha, Dose escalation stage of a first-in-class phase I study of the novel oral ERK 1/2 kinase inhibitor BVD-523 (ulixertinib) in patients with advanced solid tumors, J. Clin. Oncol. 33 (2015).
[30] S.B. Peng, J. Henry, M. Kaufman, W.P. Lu, B.D. Smith, S. Vogeti, S. Wise, Y.Y. Zhang, R. Van Horn, X.Y. Zhang, T.G. Yin, V. Yadav, L. Huber, L. Kays, J. Walgren, D. McCann, P. Patel, S. Buchanan, I. Conti, J.J. Starling, D.L. Flynn, Identification of LY3009120 as a pan inhibitor of Raf isoforms and dimers with minimal paradoxical activation and activities against BRaf or Ras mutant tumor cells, Cancer Res. 74 (2014).
[31] S.B. Peng, J.R. Henry, M.D. Kaufman, W.P. Lu, B.D. Smith, S. Vogeti, T.J. Rutkoski, S. Wise, L. Chun, Y.Y. Zhang, R.D. Van Horn, T.G. Yin, X.Y. Zhang, V. Yadav, S.H. Chen, X.Q. Gong, X.W. Ma, Y. Webster, S. Buchanan, I. Mochalkin, L. Huber, L. Kays, G.P. Donoho, J. Walgren, D. McCann, P. Patel, I. Conti, G.D. Plowman, J.J. Starling, D.L. Flynn, Inhibition of RAF Isoforms and active dimers by LY3009120 leads to anti-tumor activities in RAS or BRAF mutant cancers, Cancer Cell 28 (2015) 384–398.
[32] R.L. Kortum, D.K. Morrison, Path forward for RAF therapies: inhibition of monomers and dimers, Cancer Cell 28 (2015) 279–281.
[33] A. Zanzoni, L. Montecchi-Palazzi, M. Quondam, G. Ausiello, M. Helmer-Citterich, G. Cesareni, MINT: a Molecular INTeraction database, Febs Lett. 513 (2002) 135–140.
[34] H. Hermjakob, L. Montecchi-Palazzi, G. Bader, R. Wojcik, L. Salwinski, A. Ceol, S. Moore, S. Orchard, U. Sarkans, C. von Mering, B. Roechert, S. Poux, E. Jung, H. Mersch, P. Kersey, M. Lappe, Y.X. Li, R. Zeng, D. Rana, M. Nikolski, H. Husi, C. Brun, K. Shanker, S.G.N. Grant, C. Sander, P. Bork, W.M. Zhu, A. Pandey, A. Brazma, B. Jacq, M. Vidal, D. Sherman, P. Legrain, G. Cesareni, L. Xenarios, D. Eisenberg, B. Steipe, C. Hogue, R. Apweiler, The HUPOPSI's Molecular Interaction format - a community standard for the representation of protein interaction data, Nat. Biotechnol. 22 (2004) 177–183.
[35] C. Stark, B.J. Breitkreutz, T. Reguly, L. Boucher, A. Breitkreutz, M. Tyers, BioGRID: a general repository for interaction datasets, Nucleic Acids Res. 34 (2006) D535–D539.
[36] X. Lu, V.V. Jain, P.W. Finn, D.L. Perkins, Hubs in biological interaction networks exhibit low changes in expression in experimental asthma, Mol. Syst. Biol. 3 (2007).
[37] H. Hermjakob, L. Montecchi-Palazzi, C. Lewington, S. Mudali, S. Kerrien, S. Orchard, M. Vingron, B. Roechert, P. Roepstorff, A. Valencia, H. Margalit, J. Armstrong, A. Bairoch, G. Cesareni, D. Sherman, R. Apweiller, IntAct: an open source molecular interaction database, Nucleic Acids Res. 32 (2004) D452–D455.
[38] J.R. Henry, M.D. Kaufman, S.B. Peng, Y.M. Ahn, T.M. Caldwell, L. Vogeti, H. Telikepalli, W.P. Lu, M.M. Hood, T.J. Rutkoski, B.D. Smith, S. Vogeti, D. Miller, S.C. Wise, L. Chun, X.Y. Zhang, Y.Y. Zhang, L. Kays, P.A. Hipskind, A.D. Wrobleski, K.L. Lobb, J.M. Clay, J.D. Cohen, J.L. Walgren, D. McCann, P. Patel, D.K. Clawson, S. Guo, D. Manglicmot, C. Groshong, C. Logan,

Please cite this article in press as: Y. Chen, et al., Integrated bioinformatics, computational and experimental methods to discover novel Raf/extracellular-signal regulated kinase (ERK) dual inhibitors against breast cancer cells, European Journal of Medicinal Chemistry (2016), http://dx.doi.org/10.1016/j.ejmech.2016.11.009

J.J. Starling, D.L. Flynn, Discovery of 1-(3,3-Dimethylbutyl)-3-(2-fluoro-4-methyl-5-(7-methyl-2-(methylamino)py rido 2,3-d pyrimidin-6-yl)phenyl) urea (LY3009120) as a Pan-RAF inhibitor with minimal paradoxical activation and activity against BRAF or RAS mutant tumor cells, J. Med. Chem. 58 (2015) 4165–4179.

[39] S. Ma, L.L. Yang, T. Niu, C. Cheng, L. Zhong, M.W. Zheng, Y. Xiong, L.L. Li, R. Xiang, L.J. Chen, Q. Zhou, Y.Q. Wei, S.Y. Yang, SKLB-677, an FLT3 and Wnt/beta-catenin Signaling Inhibitor, Displays Potent Activity in Models of FLT3-driven AML, Scientific Reports, 2015, p. 5.

[40] Y.L. Pan, M.W. Zheng, L. Zhong, J. Yang, S. Zhou, Y. Qin, R. Xiang, Y.Z. Chen, S.Y. Yang, A preclinical evaluation of SKLB261, a multikinase inhibitor of EGFR/src/VEGFR2, as a therapeutic agent against pancreatic Cancer, Mol. Cancer Ther. 14 (2015) 407–418.

[41] C.H. Zhang, M.W. Zheng, Y.P. Li, X.D. Lin, M. Huang, L. Zhong, G.B. Li, R.J. Zhang, W.T. Lin, Y. Jiao, X.A. Wu, J. Yang, R. Xiang, L.J. Chen, Y.L. Zhao, W. Cheng, Y.Q. Wei, S.Y. Yang, Design, synthesis, and structure-activity relationship studies of 3-(Phenylethynyl)-1H-pyrazolo 3,4-d pyrimidin-4-amine derivatives as a new class of src inhibitors with potent activities in models of triple negative breast Cancer, J. Med. Chem. 58 (2015) 3957–3974.

Please cite this article in press as: Y. Chen, et al., Integrated bioinformatics, computational and experimental methods to discover novel Raf/extracellular-signal regulated kinase (ERK) dual inhibitors against breast cancer cells, European Journal of Medicinal Chemistry (2016), http://dx.doi.org/10.1016/j.ejmech.2016.11.009